Article

Immunity

Inflammatory Ly6C^{high} Monocytes Protect against Candidiasis through IL-15-Driven NK Cell/Neutrophil Activation

Graphical Abstract

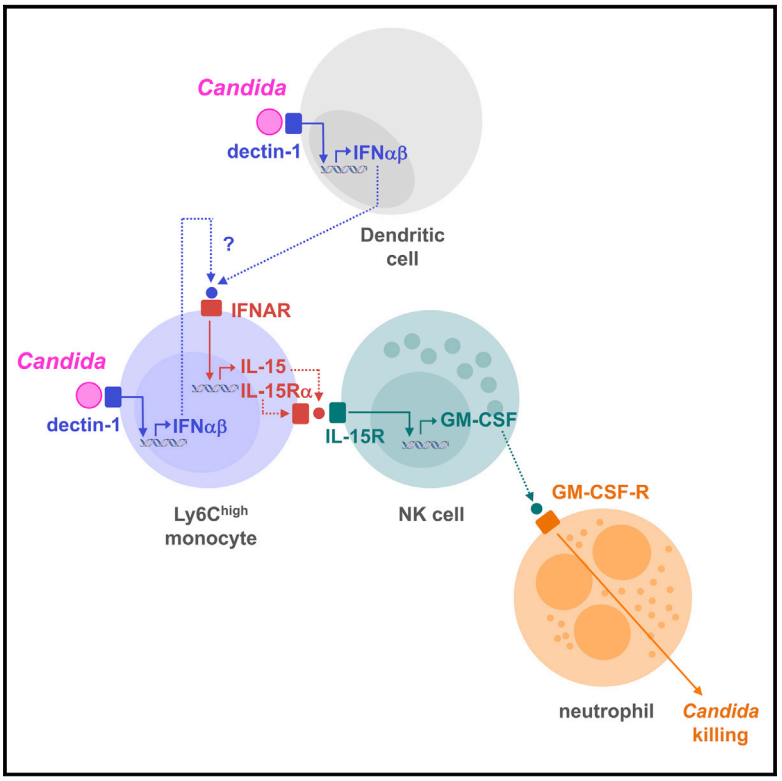

Highlights

- NK cell and neutrophil activation during *C. albicans* infection requires IL-15
- Inflammatory Ly6C^{high} monocytes are the main source of IL-15 in response to *C. albicans* infection
- Type I IFN controls *C. albicans*-induced IL-15 production by inflammatory monocytes
- Defense against systemic candidiasis requires spleen-kidney cooperative immunity

Authors

Jorge Domínguez-Andrés, Lidia Feo-Lucas, María Minguito de la Escalera, Leticia González, María López-Bravo, Carlos Ardavín

Correspondence

ardavin@cnb.csic.es

In Brief

The kidney is the main target organ in systemic *C. albicans* infection. Domínguez-Andrés et al. now show that effective defense against systemic candidiasis relies on type I interferon-dependent IL-15 production by spleen inflammatory monocytes, which drives splenic NK cell activation and GM-CSF release that in turn boost the candidacidal potential of kidney neutrophils.

Domínguez-Andrés et al., 2017, Immunity *46*, 1059–1072
June 20, 2017
http://dx.doi.org/10.1016/j.immuni.2017.05.009

CellPress

Immunity
Article

Inflammatory Ly6C^{high} Monocytes Protect against Candidiasis through IL-15-Driven NK Cell/Neutrophil Activation

Jorge Domínguez-Andrés,[1] Lidia Feo-Lucas,[1] María Minguito de la Escalera,[1] Leticia González,[1] María López-Bravo,[1] and Carlos Ardavín[1,2,*]
[1]Departamento de Inmunología y Oncología, Centro Nacional de Biotecnología/CSIC, Darwin 3, 28049 Madrid, Spain
[2]Lead contact
*Correspondence: ardavin@cnb.csic.es
http://dx.doi.org/10.1016/j.immuni.2017.05.009

SUMMARY

Neutrophils play a crucial role in defense against systemic candidiasis, a disease associated with a high mortality rate in patients receiving immunosuppressive therapy, although the early immune mechanisms that boost the candidacidal activity of neutrophils remain to be defined in depth. Here, we used a murine model of systemic candidiasis to explore the role of inflammatory Ly6C^{high} monocytes in NK cell-mediated neutrophil activation during the innate immune response against *C. albicans*. We found that efficient anti-*Candida* immunity required a collaborative response between the spleen and kidney, which relied on type I interferon-dependent IL-15 production by spleen inflammatory Ly6C^{high} monocytes to drive efficient activation and GM-CSF release by spleen NK cells; this in turn was necessary to boost the *Candida* killing potential of kidney neutrophils. Our findings unveil a role for IL-15 as a critical mediator in defense against systemic candidiasis and hold promise for the design of IL-15-based antifungal immunotherapies.

INTRODUCTION

Candida species are the most common cause of fungal infection in immunocompromised patients. Systemic candidiasis can lead to severe life-threatening invasive disease in patients receiving immunosuppressive therapy for autoimmune diseases or organ transplantation, and in those with neoplastic disease, AIDS, or undergoing major surgery. The incidence of invasive candidiasis has risen dramatically over the past decades and this disease is associated with a high mortality rate, exceeding 40% (Kullberg and Arendrup, 2015). Current therapies for invasive candidiasis, based on the use of antifungal drugs, have low efficacy in immunocompromised patients, and the emergence of resistance to antifungal agents is becoming a major concern (Kanafani and Perfect, 2008). A growing body of evidence supports the notion that the design of effective therapies against fungal infections requires the development of immunotherapeutic strategies, which could be combined with antifungal chemotherapy. However, despite intense research efforts, the development of efficient antifungal immunotherapies has fallen behind in part due to an insufficient understanding of the host-pathogen interactions involved and the mechanisms underlying the induction of protective immunity or immune escape during fungal infections.

Defense against fungal infections relies to a great extent on the activation of neutrophils, a process sequentially controlled first by the innate immune response and subsequently by the adaptive branch of antifungal immunity (Netea et al., 2015). Whereas neutrophil recruitment and activation during antifungal adaptive immunity has been analyzed in-depth (Hernández-Santos and Gaffen, 2012), few studies have attempted to unravel the innate immune mechanisms that boost the candidacidal activity of neutrophils during the early phases of fungal infection. Interestingly, a recent report demonstrated that NK cells, generally associated with anti-viral, anti-bacterial, or anti-tumoral immunity, play a crucial role in the early defense against systemic *Candida albicans* infection in mice through the production of the cytokine GM-CSF, which is required for the activation of neutrophils in this infection model (Bär et al., 2014). Whereas this report represents a groundbreaking contribution to the field, it also led to several yet unsolved questions related to NK cell and neutrophil activation during the early anti-*Candida* innate immune response. Which are the cells and mediators responsible for this early NK cell activation? Where do NK cell-activating cells encounter and respond to infection? Where are NK cells and neutrophils activated during the early phases of systemic candidiasis? In this regard, by using a model of inducible diphtheria-toxin-mediated monocyte depletion Ngo et al., have reported that inflammatory Ly6C^{high} monocytes are critical during the first 48 hr after *C. albicans* infection for the induction of a protective response (Ngo et al., 2014). In line with this finding, recent reports have also highlighted the functional relevance of inflammatory Ly6C^{high} monocytes in the induction of the early phases of innate immunity against microbial infections (Soudja et al., 2012; Xiong et al., 2016).

These studies prompted us to explore the role of inflammatory Ly6C^{high} monocytes in the activation of the NK cell-neutrophil axis during the early innate immune response against *C. albicans*, using a murine model of systemic candidiasis in which the kidney is the main target organ (Lionakis et al., 2011). We found that during *C. albicans* infection, the production of IL-15 by spleen inflammatory Ly6C^{high} monocytes was

needed for an efficient activation and production of GM-CSF by spleen NK cells, which in turn was required to boost the *Candida* killing potential of neutrophils. IL-15 production by Ly6C^{high} monocytes was strictly dependent on type I interferon (IFN) production, which had a crucial role in defense against *C. albicans* infection (del Fresno et al., 2013). Thus, IL-15 plays a critical function in the activation of the NK cell-neutrophil axis during systemic candidiasis and defense against *Candida* relies on the induction of spleen-kidney cooperative innate immunity wherein the production of IL-15 and activation of NK cells in the spleen enables an efficient GM-CSF-dependent activation of neutrophils and the clearance of *Candida* in the kidney. These findings provide a basis for the design of IL-15-based immunotherapeutic strategies for the treatment of invasive candidiasis affecting immunocompromised patients.

RESULTS

Characterization of Kidney and Spleen DC, Monocyte, and Macrophage Subsets during Systemic *C. albicans* Infection

We first performed, in non-infected C57BL/6 mice, a detailed analysis of the different subsets of dendritic cells (DCs), monocytes and macrophages (MØs) present in the kidney, the main target organ after systemic *C. albicans* infection. Kidney cell suspensions obtained after enzymatic digestion were analyzed by 7-color flow cytometry. After gating on CD45^{+} cells, and exclusion of cells expressing CD90 (T cells), CD19 (B cells), CD49b (NK cells), Siglec-F (eosinophils), or Ly6G (neutrophils), a sequential gating strategy based on the differential expression of CD11b, CD64, Ly6C, MHCII, and CD11c (Figure S1), allowed for the characterization of kidney-resident MØs, Ly6C^{low} and Ly6C^{high} monocytes, monocyte-derived DCs (moDCs), and conventional DCs (cDCs). In addition, CD64^{int}, CD11b^{high} immature moDCs (i-moDCs), co-expressing Ly6C and MHCII, can be defined in non-infected mice, although this population was more prominent 24 hr after *C. albicans* infection (Figure 1A). NK cells and neutrophils were identified as CD49b^{+} CD3^{-} cells, and Ly6G^{+} cells, respectively (Figure S1).

We next analyzed the kinetics of these cell subsets in the kidney during the first 48 hr after infection (Figures 1A and 1B), since innate immunity mechanisms against *C. albicans* are triggered during the first hours of infection (Netea et al., 2008). During the first 24 hr post-infection large numbers of Ly6C^{high} monocytes and neutrophils were recruited to the kidney. Along the next 24 hr the recruitment of Ly6C^{high} monocytes and neutrophils continued and was accompanied by the recruitment of large numbers of Ly6C^{low} monocytes. As a consequence, the number of Ly6C^{low}, Ly6C^{high} monocytes, and neutrophils increased around 50-, 100-, and 150-fold, respectively, during the first 48 hr. The number of NK cells recruited to the kidney also increased substantially during the first 24 hr post-infection. In contrast, during the first 48 hr the number of resident macrophages (res-MØs) remained unchanged, and cDCs underwent just a moderate increase in number. At 48 hr the number of moDCs was more than 10-fold lower than the number of Ly6C^{high} monocytes (Figure 1B), suggesting that the differentiation of Ly6C^{high} monocytes into moDCs was limited by the infection process. This hypothesis was supported by the low number of i-moDCs at 48 hr post-infection, and by the fact that the decreased expression of Ly6C in Ly6C^{high} monocytes was not concomitant with the increased expression of MHCII (Figure 1A).

Since the spleen fulfills an important function against systemic infections and is transiently infected by *C. albicans* during the first hours after infection (Lionakis et al., 2011), we analyzed the kinetics of recruitment of DCs, monocytes, and MØs to the spleen during the first 48 hr after *C. albicans* infection. There was a significant increase in the number of Ly6C^{high} monocytes and neutrophils (around 3- and 10-fold respectively at 48 hr) in the spleen, but not of Ly6C^{low} monocytes (Figures S1, 2A and 2B). Although the increase in the number of monocytes and neutrophils was lower in the spleen than in the kidney, it is important to note that the size of these cell populations was significantly higher in the spleen both at 24 and 48 hr post-infection (Figures 1B and 2B). Consequently, during the first hours of infection, Ly6C^{high} monocytes and neutrophils were rapidly recruited to the kidney and spleen, the latter harboring a substantially higher number of both cell types. In contrast, the number of spleen NK cells remained unchanged during the first 24 hr, but underwent a significant reduction from 24 to 48 hr. Importantly, the size of the NK cell population was around 100-fold higher in the spleen than in the kidney (Figures 1B and 2B).

CCR2 Deficiency Increases Susceptibility to Systemic *C. albicans* Infection

To explore the contribution of monocytes to the early innate immune response against *Candida*, we initially analyzed the kinetics of DCs, monocytes, MØs, NK cells, and neutrophils in the kidney and spleen after *C. albicans* infection in mice deficient for CCR2 (*Ccr2*$^{-/-}$ mice), a chemokine receptor controlling the egress of Ly6C^{high} monocytes from the bone marrow, and thus their recruitment to inflammatory foci (Shi and Pamer, 2011). The number of res-MØs, Ly6C^{low} monocytes, and cDCs were not significantly affected in the kidney of *Ccr2*$^{-/-}$ mice (Figure 1C and 1D). However, a large reduction in Ly6C^{high} monocytes numbers was observed in the kidney of *Ccr2*$^{-/-}$ mice at 24 hr post-infection, which was paralleled by a moderate reduction in the size of the moDC population and by lower neutrophil recruitment. At 48 hr the number of Ly6C^{high} monocytes was similar in wild-type (WT) and *Ccr2*$^{-/-}$ mice, indicating that the blockade in monocyte recruitment was reverted by 48 hr post-infection. No significant differences were observed in the number of kidney moDCs and neutrophils at 48 hr between WT and *Ccr2*$^{-/-}$ mice. CCR2 deficiency affected similarly the kinetics of Ly6C^{high} monocytes, moDCs, and neutrophils in the spleen at 24 and 48 hr post infection and led to a significant reduction in the number of cDCs (Figure 2C and 2D).

We next analyzed the impact on defense against *C. albicans*, of the reduction primarily in the number of Ly6C^{high} monocytes, and additionally in moDCs, cDCs and neutrophils, occurring in the kidney and spleen of *Ccr2*$^{-/-}$ mice during the first 48 hr. *Ccr2*$^{-/-}$ mice harbored a significantly higher renal fungal load at 24 hr post-infection than control mice, and this difference in fungal load was more prominent at 48 hr (Figure 3A). Correspondingly, the size of renal leukocytic infiltrates and growth of *Candida* hyphae, as assessed in histological sections, was significantly higher in *Ccr2*$^{-/-}$ mice (Figure S2), whereas the survival was significantly higher in WT mice (Figure 3B). Analysis of

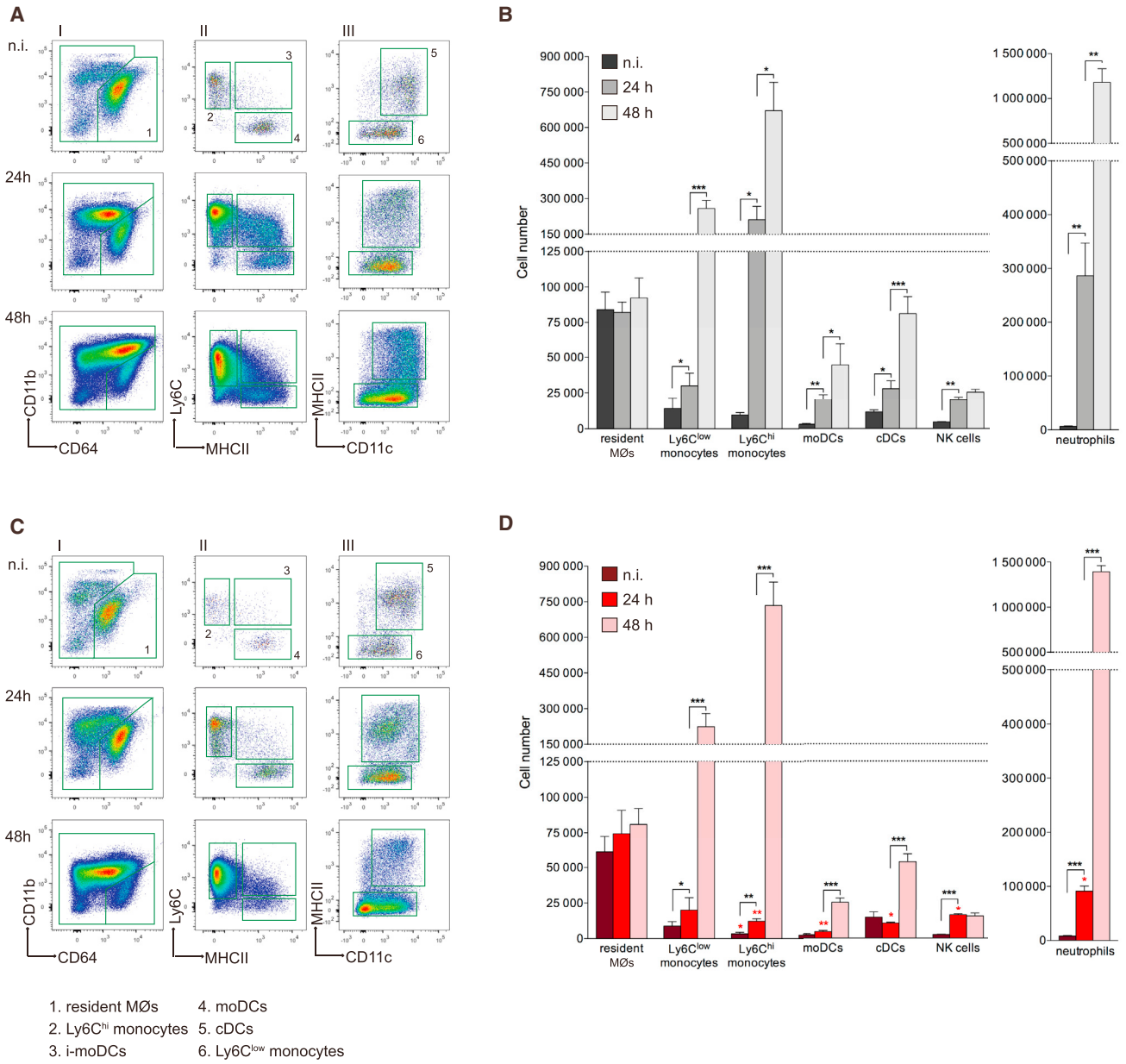

Figure 1. Kinetics of Kidney DC, Monocyte, MØ, NK Cell, and Neutrophil Subsets during Systemic *C. albicans* Infection of WT and *Ccr2*$^{-/-}$ Mice

(A and C) Flow cytometry analysis of kidney DC, monocyte, MØ, NK cell, and neutrophil subsets (defined as described in Figure S1) before and after infection in WT (A) and *Ccr2*$^{-/-}$ mice (C).

(B and D) Absolute cell number per mouse of the indicated kidney cell subsets after infection, in WT (B) and *Ccr2*$^{-/-}$ mice (D). Data are expressed as mean ± SEM of four mice per condition. *p < 0.05; **p < 0.01; ***p < 0.001; unpaired t test. Red asterisks indicate the statistical significance of the differences between WT and *Ccr2*$^{-/-}$ mice. Similar results were obtained in at least three independent experiments. See also Figure S1.

the *C. albicans* killing ability of blood neutrophils revealed that whereas in control mice a significant increase in neutrophil killing potential occurred during the first 48 hr, in *Ccr2*$^{-/-}$ mice the killing ability of neutrophils was not significantly increased during infection (Figure 3C). Consequently, after infection, blood neutrophils from WT mice acquired a higher candidacidal potential than their *Ccr2*$^{-/-}$ counterparts. In line with these data, neutrophils isolated from the kidney of control mice 48 hr post infection had a significantly higher *C. albicans* killing ability than those isolated from *Ccr2*$^{-/-}$ mice (Figure 3C), and displayed a higher amount of mRNA transcripts encoding the enzyme inducible nitric oxide synthase (iNOS; Figure 3D), which catalyzes the production of nitric oxide, a strong candidacidal molecule (Naglik, 2014). Accordingly, iNOS mRNA expression by MACS-sorted CD45^{+} kidney infiltrating leukocytes was increased during the first 48 hr post-infection in WT but not in *Ccr2*$^{-/-}$ mice

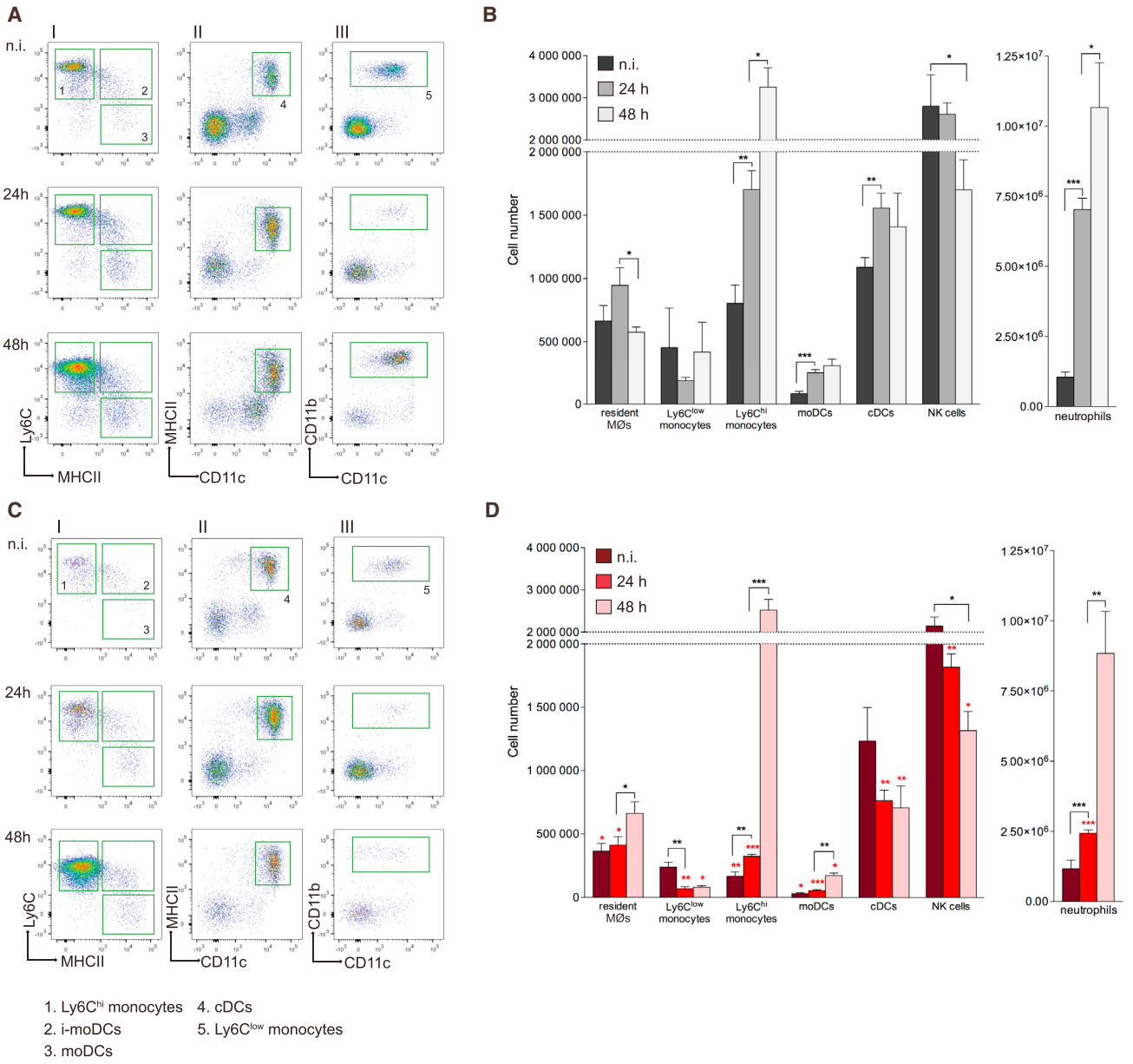

Figure 2. Kinetics of Spleen DC, Monocyte, MØ, NK Cell, and Neutrophil Subsets during Systemic *C. albicans* Infection of WT and *Ccr2*$^{-/-}$ Mice

(A and C) Flow cytometry analysis of spleen DC, monocyte, MØ, NK cell, and neutrophil subsets (defined as described in Figure S1) before and after infection, in WT (A) and *Ccr2*$^{-/-}$ mice (C).

(B and D) Absolute cell number per mouse of the indicated spleen cell subsets after infection, in WT (B) and *Ccr2*$^{-/-}$ mice (D). Data are expressed as mean ± SEM of four mice per condition. *$p < 0.05$; **$p < 0.01$; ***$p < 0.001$; unpaired t test. Red asterisks indicate the statistical significance of the differences between WT and *Ccr2*$^{-/-}$ mice. Similar results were obtained in at least three independent experiments. See also Figure S1.

(Figure 3D). Therefore, during the first 48 hr post-infection, the higher *Candida* killing ability of neutrophils from WT mice, as compared to that of *Ccr2*$^{-/-}$ mice, correlated with a lower kidney fungal burden and a prolonged survival.

As pointed out above, GM-CSF production by NK cells is crucial to boost the candidacidal potential of neutrophils (Bär et al., 2014). We therefore sought to assess whether in *Ccr2*$^{-/-}$ mice, the decreased *Candida* killing ability of neutrophils reflected the production of lower amounts of GM-CSF by NK cells. ELISA analysis of GM-CSF levels in blood serum showed that *Ccr2*$^{-/-}$ mice produced lower amounts of GM-CSF than their WT counterparts both at 24 and at 48 hr post-infection (Figure 3E). In addition, these experiments revealed that higher serum GM-CSF levels were detectable at 24 hr than at 48 hr. In line with these findings, the expression of GM-CSF-specific mRNA by MACS-sorted CD45^{+} kidney-infiltrating leukocytes and by MACS-sorted CD11b^{+} spleen cells (including NK cells and myeloid cells) from WT mice was higher at 24 than at 48 hr

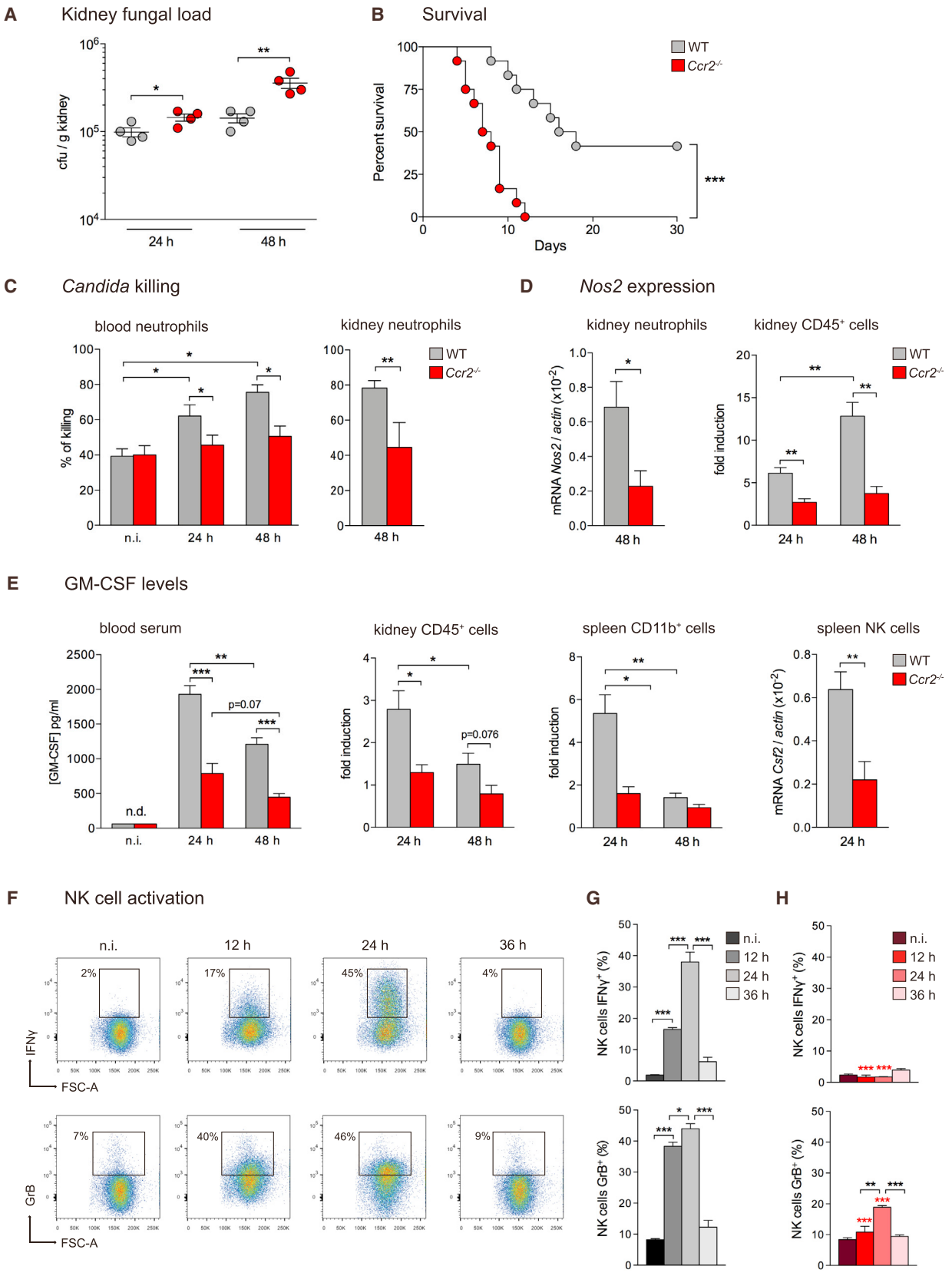

(legend on next page)

mice (Figure 3E). Importantly, at 24 hr post-infection GM-CSF mRNA expression was significantly lower in the kidney and spleen of *Ccr2*$^{-/-}$. Because NK cells were reported to be the main GM-CSF producers during *C. albicans* infection (Bär et al., 2014) and because the size of the NK cell population before and after *C. albicans* infection was around 100-fold higher in the spleen than in the kidney (Figures 1B and 2B), our data support the notion that the higher levels of GM-CSF observed in WT versus *Ccr2*$^{-/-}$ mice most likely reflect a lower GM-CSF production by spleen NK cells in *Ccr2*$^{-/-}$ mice in response to *C. albicans*. In support of this hypothesis, a lower expression of GM-CSF mRNA was detected in spleen MACS-sorted NK cells from *Ccr2*$^{-/-}$ mice as compared to their WT counterparts (Figure 3E). Thus, our results suggest that GM-CSF was primarily produced by spleen NK cells during the first 24 hr post-infection, and its production was significantly lower in *Ccr2*$^{-/-}$ mice. In line with this hypothesis, the number of NK cells harbored by the spleen was significantly lower in *Ccr2*$^{-/-}$ mice at 24 and 48 hr post-infection (Figures 2B and 2D).

Finally, we sought to determine whether the lower amounts of GM-CSF mRNA expressed by NK cells in *Ccr2*$^{-/-}$ mice correlated with the decreased NK cell activation during *C. albicans* infection. For this purpose, the synthesis of IFN-γ and granzyme B by spleen NK cells was analyzed in WT and *Ccr2*$^{-/-}$ mice by flow cytometry after intracellular staining. At 24 hr post-infection, approximately 40% of spleen NK cells stained positive for IFN-γ and granzyme B, whereas IFN-γ^{+} cells were no longer detectable at 36 hr (Figure 3F and 3G). Analyses of spleen NK cells from *Ccr2*$^{-/-}$ mice revealed no detectable IFN-γ production and significantly reduced granzyme B production, indicating that NK cell activation was defective after *C. albicans* infection of *Ccr2*$^{-/-}$ mice (Figure 3H). In addition, kidney NK cells were poorly activated after *C. albicans* infection of either WT or *Ccr2*$^{-/-}$ mice, indicating that the ability of these cells to produce GM-CSF during *C. albicans* infection was limited (Figure S3). Therefore, it can be hypothesized that in *Ccr2*$^{-/-}$ mice, poor NK cell activation led to reduced GM-CSF production, which in turn compromised the candidacidal ability of neutrophils and resulted in a higher kidney fungal load and a lower survival.

IL-15 Is Selectively Produced by Inflammatory Monocytes during *C. albicans* Infection

A number of cytokines, such as IL-2, IL-12 (a heterodimer composed of IL-12p40 and IL-12 p35), IL-15, IL-18, or IL-23 (a heterodimer composed of IL-12p40 and IL-23p19) have been reported to control NK cell activation during infectious processes (Horowitz et al., 2012; Marçais et al., 2013). Thus, we next analyzed whether the defective induction of NK cell activation in *Ccr2*$^{-/-}$ mice could result from a deficient production of these cytokines during *C. albicans* infection. For this purpose, the expression of mRNA for IL-2, IL-12p40, IL-12 p35, IL-15, IL-18, and IL-23p19 was analyzed at 24 and 48 hr post-infection in MACS-sorted CD11b^{+} spleen cells and MACS-sorted CD45^{+} kidney infiltrating leukocytes from WT mice and *Ccr2*$^{-/-}$ mice. Our data revealed that the transcription of mRNA for all these cytokines was induced by *C. albicans* infection in CD11b^{+} spleen cells (Figure 4A) and CD45^{+} kidney infiltrating leukocytes (Figure 4B). No differences were observed between the two genotypes for all the cytokines analyzed with the exception of IL-15, which was markedly increased at 24 hr both in the spleen and kidney in WT, but not in *Ccr2*$^{-/-}$ mice. These results suggest that at 24 hr post-infection, in *Ccr2*$^{-/-}$ mice the production of IL-15, a key cytokine for the development and function of NK cells (Di Santo, 2006), was compromised most likely due to a defective recruitment and/or development of a CCR2-dependent cell population, in the spleen and/or the kidney.

To confirm this hypothesis, we assessed which were the main IL-15 producer cells in the spleen and kidney of *C. albicans*-infected WT mice by analyzing, by flow cytometry, the expression of IL-15Rα, the IL-15 trans-presenting receptor that is coexpressed with IL-15 (Mortier et al., 2008). Our data revealed that, in the spleen, Ly6C^{high} monocytes were the main cell population expressing IL-15Rα (Figures 4C and 4D). At 24 hr, around 80% Ly6C^{high} monocytes expressed IL-15Rα, which was dramatically reduced by 48 hr post-infection. DCs (including moDCs and cDCs) and neutrophils followed similar kinetics, although only up to 10% and 5% of these cell populations, respectively, expressed IL-15Rα at 24 hr post-infection. IL-15Rα^{+} cells were not detectable among splenic resident MØs or lymphoid cells. Consequently, Ly6C^{high} monocytes represented around 80% of all spleen IL-15Rα^{+} cells, indicating that they constituted the main splenic IL-15-producing population. The kinetics of IL-15Rα expression was similar in the kidney of *C. albicans* infected mice, but only around 30% Ly6C^{high} monocytes expressed IL-15Rα at 24 hr (Figures 4E and 4F). Up to 20% kidney-resident MØs were positive for IL-15Rα, that was barely detectable among kidney DCs or neutrophils. Thus, Ly6C^{high} monocytes also constituted the main IL-15 producing cell

Figure 3. Effect of CCR2 Deficiency in Defense against Systemic *C. albicans* Infection

(A) Kidney fungal burden of WT mice and *Ccr2*$^{-/-}$ mice at 24 and 48 hr after infection.

(B) Survival of WT mice and *Ccr2*$^{-/-}$ mice after infection. Data are presented as a Kaplan-Maier plot with a log rank test used to compare susceptibility between the two groups. n = 12.

(C) Candidacidal activity of neutrophils isolated from blood and kidney of WT and *Ccr2*$^{-/-}$ mice at the indicated times after infection.

(D) Expression of mRNA for iNOS by purified kidney neutrophils and MACS-sorted CD45^{+} kidney infiltrating leukocytes analyzed by real-time PCR, normalized to β-actin, at the indicated times after infection. Data are expressed as fold induction relative to non-infected mice.

(E) GM-CSF analyzed by ELISA in blood serum, and by real-time PCR normalized to β-actin, in MACS-sorted CD45^{+} kidney infiltrating leukocytes, MACS-sorted CD11b^{+} spleen cells and purified spleen NK cells from WT and *Ccr2*$^{-/-}$ mice at the indicated times after infection. For MACS-sorted cells data are expressed as fold induction relative to non-infected mice.

(F–H) IFN-γ and Granzyme B (GrB) production by spleen NK cells analyzed by flow cytometry in WT (F and G) and *Ccr2*$^{-/-}$ mice (H) at the indicated times after infection. Data are expressed as mean ± SEM of four mice per condition. *p < 0.05; **p < 0.01; ***p < 0.001; unpaired t test. Red asterisks indicate the statistical significance of the differences observed between WT and *Ccr2*$^{-/-}$ mice. Similar results were obtained in at least three independent experiments. ELISA data for non-infected mice were below the detection level of the ELISA kit (63 pg/ml). n.i., non-infected; n.d., not detectable. See also Figures S2 and S3.

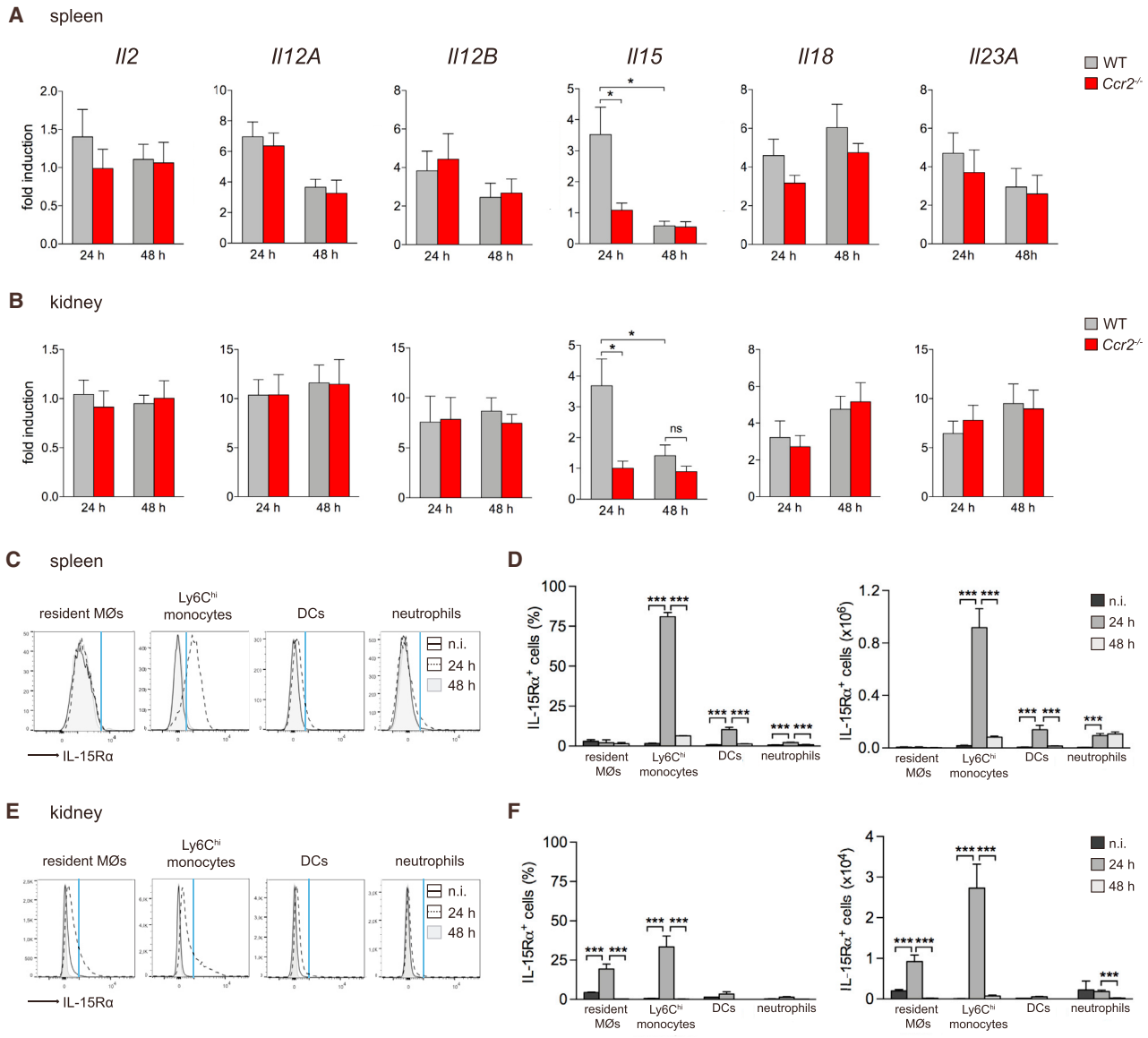

Figure 4. IL-15 Is Selectively Produced by Inflammatory Monocytes during Systemic *C. albicans* Infection

(A and B) Expression of mRNA for the indicated cytokines by spleen MACS-sorted CD11b$^+$ spleen cells (A) and MACS-sorted CD45$^+$ kidney infiltrating leukocytes (B) analyzed by real-time PCR normalized to β-actin, at the indicated times after infection. Data are expressed as fold induction relative to in non-infected mice.

(C and E) Analysis of IL-15Rα expression by flow cytometry by resident MØs, Ly6C^{hi} monocytes, DCs and neutrophils in the spleen (C) and kidney (E) of non-infected C57BL/6 mice (solid lines) and C57BL/6 mice 24 (dashed lines) and 48 hr (gray profiles) after infection.

(D and F) Quantification of the percentage and number of IL-15Rα$^+$ cells for spleen (D) and kidney (F) resident MØs, Ly6C^{hi} monocytes, DCs, and neutrophils at the indicated times after infection. Data are expressed as mean ± SEM of four mice per condition. *p < 0.05; **p < 0.01; ***p < 0.001; unpaired t test. Similar results were obtained in at least three independent experiments. See also Figures S4 and S5.

population in the kidney. However, due to the differences in size of the Ly6C^{high} monocyte population in the spleen and kidney at 24 hr post-infection, it can be concluded that spleen Ly6C^{high} monocytes were a primary source of IL-15 during *C. albicans* infection (at 24 hr the spleen harbored around 0.9 × 10^6 IL-15Rα$^+$ Ly6C^{high} monocytes while only around 3 × 10^4 IL-15Rα$^+$ Ly6C^{high} monocytes were detected in kidney). These data support that the deficient IL-15 production detected in the spleen and kidney of *C. albicans*-infected *Ccr2*$^{-/-}$ mice at 24 hr was primarily the consequence of a limited recruitment of Ly6C^{high} monocytes to these organs.

These findings suggest that during *C. albicans* infection, the production of IL-15 by inflammatory Ly6C^{high} monocytes recruited to the spleen was needed for an efficient activation and GM-CSF production by spleen NK cells, which in turn was required to boost the *Candida* killing potential of neutrophils. In line with these considerations, our data indicate that the production of IL-15 by Ly6C^{high} monocytes and the activation of NK

cells were far less efficient in the kidney than in the spleen. It is important to note that the fungal load was maintained at low levels in the spleen whereas it increased progressively in the kidney along this period (Figure S4). It can be hypothesized that the ability of the spleen to control the early phases of infection favored the induction of IL-15 production and subsequent NK cell activation, whereas the high level of infection harbored by the kidney, reflecting its low capacity to clear *Candida* during the first hours post-infection, restrained these processes.

NK Cell Activation during *C. albicans* Infection Depends on the Production of IL-15 by Ly6C^{high} Monocytes

To demonstrate that during *C. albicans* infection an efficient activation of NK cells by inflammatory Ly6C^{high} monocytes was dependent on the production of IL-15, we first assessed the impact of IL-15 deficiency on the capacity of Ly6C^{high} monocytes to activate NK cells in vitro. To this purpose, we previously confirmed the ability of Ly6C^{high} monocytes to produce IL-15 in vitro in response *C. albicans*. Our data revealed that IL-15 mRNA expression was increased after culture of bone marrow Ly6C^{high} monocytes in the presence heat-killed *C. albicans* (HKC); a similar kinetics of IL-15 mRNA expression was induced by LPS from *Escherichia coli*, a ligand of TLR4, used a positive control of IL-15 production (Figure 5A). Next we compared the ability of bone-marrow Ly6C^{high} monocytes from WT or IL-15-deficient (*Il15*$^{-/-}$) mice to activate spleen NK cells in monocyte-NK cell co-cultures in the presence of HKC or LPS. The production of GM-CSF and IFN-γ induced by HKC was severely reduced in co-cultures of NK cells with *Il15*$^{-/-}$ Ly6C^{high} monocytes compared to co-cultures of NK cells with WT Ly6C^{high} monocytes (Figure 5B), supporting that IL-15 production by Ly6C^{high} monocytes was required for spleen NK cell activation in response to *C. albicans* infection in vivo. Interestingly, GM-CSF and IFN-γ production in response to LPS was unaffected by IL-15 deficiency. Of note, neither GM-CSF nor IFN-γ production was detected after culture of NK cells or Ly6C^{high} monocytes alone.

To validate these results from in vitro experiments, we first explored the IL-15 requirement for an efficient NK cell activation during in vivo *C. albicans* infection. To this end, C57BL/6 mice were treated with an anti-IL-15Rα/IL-15 blocking mAb concomitantly with the infection with *C. albicans*, and NK cell activation was analyzed at 24 hr post-infection. Our results revealed that in mice treated with anti-IL-15/IL-15α mAb the production of IFN-γ by spleen NK cells was barely detectable and, correspondingly, the levels of GM-CSF in serum and *Candida* killing potential of neutrophils were markedly reduced, leading to an increased kidney fungal load (Figures 5C and 5D), indicating that IL-15 is a key mediator of NK cell activation during *C. albicans* infection. In this context, since, as mentioned above, IL-15 is required for NK cell development (Di Santo, 2006), *Il15*$^{-/-}$ mice, compared to their WT counterparts, had, as expected, markedly lower GM-CSF levels in serum, spleen, and kidney, paralleled with a significantly reduced iNOS expression and *Candida* killing ability of neutrophils, that led to a higher kidney fungal burden and reduced survival (Figure S5). In contrast, monocyte candidacidal potential after *Candida* infection was not affected by IL-15 deficiency (Figure S5F), revealing that IL-15 had a key role in boosting the *Candida* killing potential of neutrophils through NK cell activation, but not of Ly6C^{high} monocytes. Next, we sought to demonstrate that NK cell activation during in vivo *C. albicans* infection relied on the production of IL-15 by inflammatory Ly6C^{high} monocytes. To this purpose, we first analyzed whether the administration of IL-15 to *Ccr2*$^{-/-}$ mice rescued the deficient NK cell activation observed in these mice after *C. albicans* infection. After IL-15 treatment, the percentage of IFN-γ-producing NK cells detected in the spleen of *Ccr2*$^{-/-}$ mice reached values comparable to those of WT mice (Figures 5E and 5F). In line with this observation, in *Ccr2*$^{-/-}$ mice the levels of GM-CSF in serum and the *Candida* killing ability of blood neutrophils increased to WT mouse values after IL-15 administration. Correspondingly the renal fungal load dropped to WT values in IL-15-treated *Ccr2*$^{-/-}$ mice. These data support that IL-15 production by CCR2-dependent cells (that, based on our results shown in Figure 4C, essentially correspond to Ly6C^{high} monocytes), was crucial for an efficient NK cell and subsequent neutrophil activation. To provide a stronger support to this hypothesis, we transferred WT or *Il15*$^{-/-}$ Ly6C^{high} monocytes intravenously into *Ccr2*$^{-/-}$ mice concomitantly with infection with *C. albicans*, and splenic NK cell activation was analyzed. Interestingly, transfer of Ly6C^{high} monocytes from WT, but not from *Il15*$^{-/-}$ mice, corrected the defective NK cell activation, GM-CSF production and neutrophil *Candida* killing ability of *Ccr2*$^{-/-}$ mice, leading to a reduction of the kidney fungal burden to WT mouse values (Figures 5G and 5H). Taken together, these results strongly suport that during *C. albicans* infection, the activation of NK cells, allowing an efficient GM-CSF dependent *Candida* killing by neutrophils, was dependent on the production of IL-15 by Ly6C^{high} monocytes. In addition, the analysis of the expression of CD122 (IL-2/15Rβ, that forms, together with the common cytokine-receptor gamma-chain, the IL-15 receptor) confirmed that CD122 was expressed by NK cells but not, at detectable levels, by neutrophils (Figure S6), supporting that during *C. albicans* infection IL-15 had not a direct effect on the fungicidal potential of neutrophils. Therefore, our data demonstrate that Ly6C^{high} monocytes are crucial effector cells for anti-*Candida* innate immunity, and reveal a new function for IL-15 by demonstrating that this cytokine plays a major role in the activation of the NK cell-neutrophil axis during *C. albicans* infection.

IL-15 Production during *C. albicans* Infection Is Controlled by Type I IFN Signaling

Previous data from our group have demonstrated that dectin-1-Syk-IRF5-dependent type I IFN production is crucial for defense against *C. albicans* infection (del Fresno et al., 2013). On the other hand, the production of IL-15 in response to TLR ligands was reported to depend on signaling though the type I IFN receptor (IFNAR) (Lucas et al., 2007). These studies led us to hypothesize that IFNAR signaling might also be required for IL-15 production during *C. albicans* infection, and consequently that type I IFN production has an essential role in the control of NK cell-neutrophil activation during systemic candidiasis. To address this issue, we first sought to explore whether IL-15 production by Ly6C^{high} monocytes after *C. albicans* infection was controlled by IFNAR signaling. Analysis of IL-15 mRNA expression by Ly6C^{high} monocytes isolated from IFNAR-deficient (*Ifnar1*$^{-/-}$) mice after stimulation with HKC or LPS confirmed that induction of IL-15 was dependent on IFNAR signaling

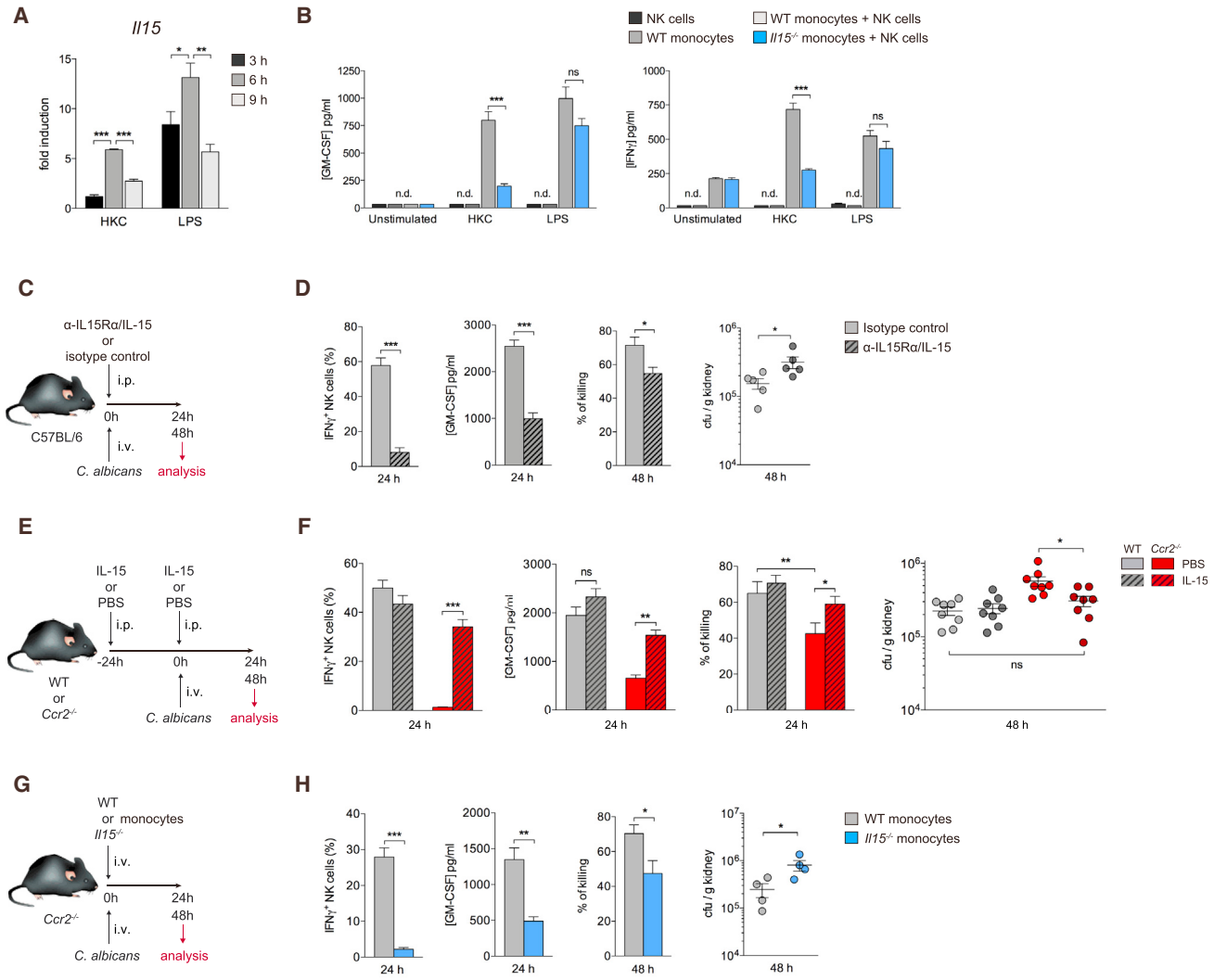

Figure 5. Role of IL-15 Production by Ly6C^{high} Monocytes in NK Cell Activation during *C. albicans* Infection

(A) Expression of mRNA for IL-15 by bone marrow monocytes from C57BL/6 mice analyzed by real-time PCR, normalized to β-actin, after stimulation with HKC or LPS. Data are expressed as fold induction relative to unstimulated cells.

(B) GM-CSF and IFN-γ production was analyzed by ELISA in cultures of NK cells or monocytes alone, or co-cultures of NK cells and WT or *Il15*$^{-/-}$ monocytes, stimulated with HKC or LPS for 16 hr.

(C) Protocol of anti-IL-15Rα/IL-15 blocking antibody treatment and *C. albicans* infection in C57BL/6 mice.

(D) Analysis of IFN-γ production by spleen NK cells by flow cytometry after intracellular staining, GM-CSF levels in blood serum by ELISA, candidacidal activity of blood neutrophils, and kidney fungal burden was performed, at the indicated times, in C57BL/6 mice treated with an anti-IL-15Rα/IL-15 blocking antibody, or an isotype control antibody, following the protocol described in (C).

(E) Protocol of recombinant IL-15 treatment and *C. albicans* infection in WT and *Ccr2*$^{-/-}$ mice.

(F) Analysis of IFN-γ production by spleen NK cells by flow cytometry after intracellular staining, GM-CSF levels in blood serum by ELISA, candidacidal activity of blood neutrophils and kidney fungal burden was performed, at the indicated times, in WT and *Ccr2*$^{-/-}$ mice treated with IL-15 or PBS, following the protocol described in (E).

(G) Protocol of WT or *Il15*$^{-/-}$ monocyte transfer and *C. albicans* infection in *Ccr2*$^{-/-}$ mice.

(H) Analysis of IFN-γ production by spleen NK cells by flow cytometry after intracellular staining, GM-CSF levels in blood serum by ELISA, candidacidal activity of blood neutrophils and kidney fungal burden was performed, at the indicated times, in *Ccr2*$^{-/-}$ mice after transfer of WT or *Il15*$^{-/-}$ monocytes and *C. albicans* infection, following the protocol described in (G). Data are expressed as mean ± SEM of four to eight mice per condition. *$p < 0.05$; **$p < 0.01$; ***$p < 0.001$; unpaired t test. Similar results were obtained in at least two independent experiments. ELISA data for unstimulated cells were below the detection level of the ELISA kits used in this study (63 pg/ml for GM-CSF and 31.6 pg/ml for IFN-γ). i.v. intravenous; n.d., not detectable. See also Figure S6.

(Figure 6A). Since the production of type I IFN in response to *C. albicans* was reported to be dectin-1 and IRF5-dependent (del Fresno et al., 2013), IL-15 mRNA induction was, as expected, blocked in dectin-1 or IRF-5-deficient bone marrow-derived DCs, after in vitro stimulation with HKC and Curdlan, a dectin-1 (*Clec7a*) ligand, but not after incubation with LPS

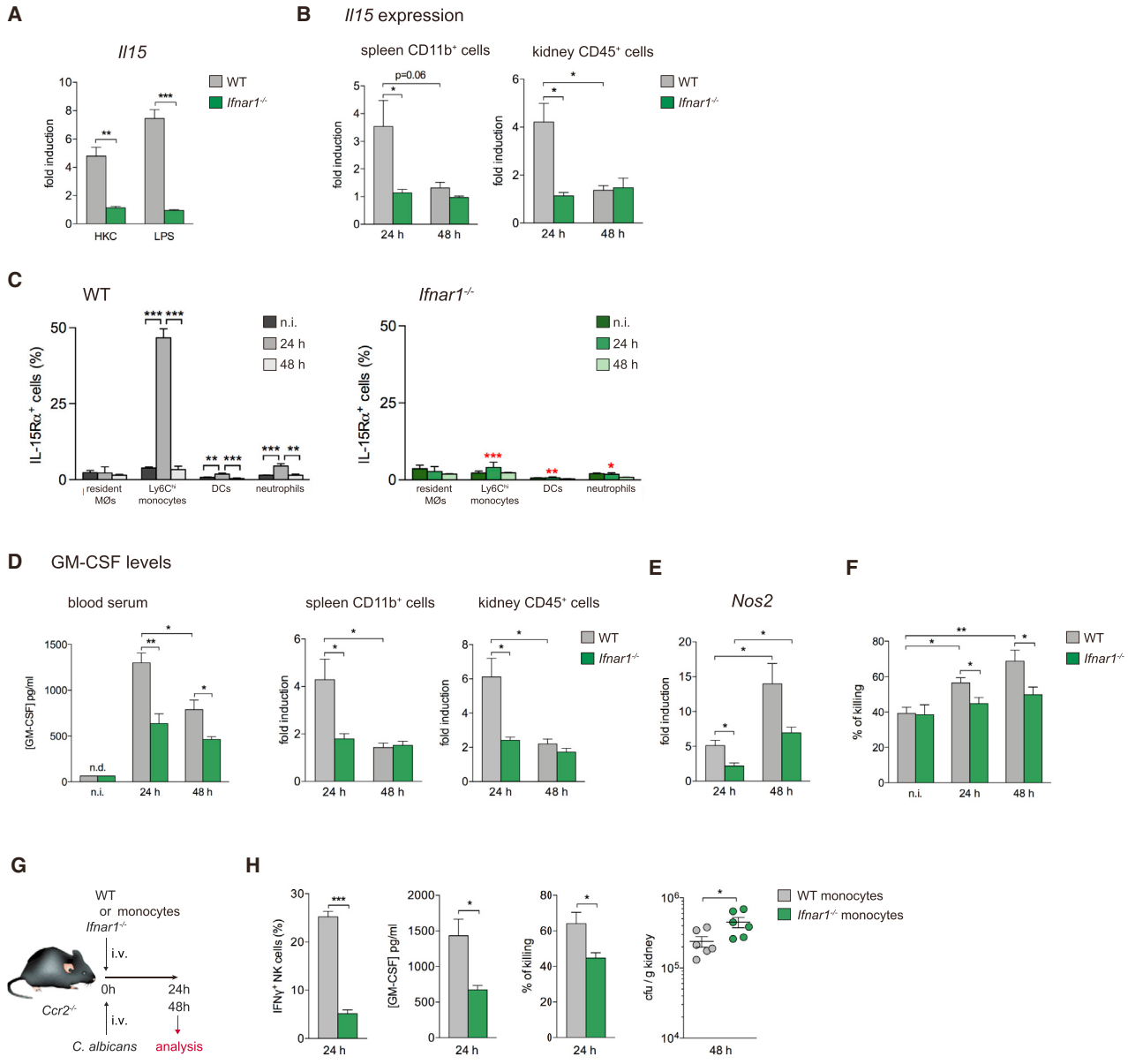

Figure 6. IL-15 Production during *C. albicans* Infection Is Controlled by Type I IFN Signaling

(A) Expression of mRNA for IL-15 by bone marrow monocytes from WT and *Ifnar*$^{-/-}$ mice analyzed by real-time PCR, normalized to β-actin, 6 hr after stimulation with HKC or LPS. Data are expressed as fold induction relative to unstimulated cells.

(B) Expression of mRNA for IL-15 by MACS-sorted CD11b^{+} spleen cells and MACS-sorted CD45^{+} kidney infiltrating leukocytes, from WT and *Ifnar*$^{-/-}$ mice, analyzed by real-time PCR normalized to β-actin, at the indicated times after infection. Data are expressed as fold induction relative to non-infected mice.

(C) Quantification of the percentage of IL-15Rα^{+} cells for spleen resident MØs, Ly6C^{hi} monocytes, DCs and neutrophils of WT and *Ifnar1*$^{-/-}$ mice, at the indicated times after infection. Red asterisks indicate the statistical significance of the differences between WT and *Ifnar1*$^{-/-}$ mice.

(D) GM-CSF analyzed by ELISA in blood serum, and by real-time PCR normalized to β-actin in MACS-sorted CD11b^{+} spleen cells and MACS-sorted CD45^{+} kidney infiltrating leukocytes, from WT and *Ifnar*$^{-/-}$ mice at the indicated times after infection. Real-time PCR data are expressed as fold induction relative to non-infected mice.

(E) Expression of mRNA for iNOS by MACS-sorted CD45^{+} kidney infiltrating leukocytes, from WT and *Ifnar*$^{-/-}$ mice analyzed by real-time PCR, normalized to β-actin, at the indicated times after infection. Real-time PCR data are expressed as fold induction relative to non-infected mice.

(F) Candidacidal activity of blood neutrophils isolated from WT and *Ifnar*$^{-/-}$ mice at the indicated times.

(G) Protocol of WT or *Ifnar1*$^{-/-}$ monocyte transfer and *C. albicans* infection in *Ccr2*$^{-/-}$ mice.

(H) Analysis of IFN-γ production by spleen NK cells by flow cytometry after intracellular staining, GM-CSF levels in blood serum by ELISA, candidacidal activity of blood neutrophils, and kidney fungal burden was performed, at the indicated times, in *Ccr2*$^{-/-}$ mice after transfer of WT or *Ifnar1*$^{-/-}$ monocytes and *C. albicans* infection, following the protocol described in (F). Data are expressed as mean ± SEM of four to six mice per condition. *p < 0.05; **p < 0.01; ***p < 0.001; unpaired t test. Similar results were obtained in at least two independent experiments. ELISA data for non-infected mice were below the detection level of the ELISA kit used (63 pg/ml). n.i., non-infected; n.d., not detectable. See also Figure S7.

(Figure S7). Interestingly, no induction of IL-15 was detectable in CD11b$^+$ spleen cells or CD45$^+$ kidney infiltrating leukocytes after *C. albicans* infection of *Ifnar1*$^{-/-}$ mice (Figure 6B). Flow cytometry analysis of splenic resident MØs, Ly6C^{high} monocytes, DCs and neutrophils confirmed that IL-15Rα was not detectable at the protein level in *Ifnar1*$^{-/-}$ mice (Figure 6C). In line with these data, the production of GM-CSF, induction of iNOS in kidney infiltrating leukocytes and candidacidal potential of neutrophils were strongly inhibited in *C. albicans*-infected *Ifnar1*$^{-/-}$ mice (Figures 6D–6F). Globally, these findings demonstrate that during *C. albicans* infection, IL-15 production by inflammatory monocytes is strictly dependent on IFNAR signaling. Interestingly, the transfer of Ly6C^{high} monocytes from WT, but not from *Ifnar1*$^{-/-}$ mice, rescued the defective NK cell activation, GM-CSF production and neutrophil *Candida* killing ability of *Ccr2*$^{-/-}$ mice, leading to a reduction of the kidney fungal burden to WT mouse values (Figures 6G and 6H). These data confirmed that during *Candida* infection, IFNAR signaling in Ly6C^{high} monocytes is required for an effective activation of the NK cell-neutrophil axis and thus protection against systemic candidiasis. Globally, these experiments further reinforce the concept that type I IFN production is crucial for defense against systemic candidiasis.

Spleen-Kidney Cooperation during Systemic *C. albicans* Infection

In mice, the kidney is the main target organ after systemic candidiasis, and therefore clearance of *Candida* requires that neutrophils recruited to the kidney perform efficiently their candidacidal function (Netea et al., 2015). On the other hand, our results reveal that defense against *C. albicans* requires the release of IL-15 by spleen inflammatory monocytes that triggers the production, primarily by spleen NK cells, of GM-CSF, reported to be required to boost the *Candida* killing potential of neutrophils (Bär et al., 2014). Therefore, our results support that innate immunity against *C. albicans* infection relies on the induction of cooperative defense mechanisms involving the spleen and kidney. It can be hypothesized that the production of IL-15 by spleen inflammatory monocytes, and subsequent activation of large numbers of spleen NK cells followed by the production of high levels of GM-CSF, would be required for an efficient induction of the candidacidal ability of neutrophils involved in *Candida* clearance in the kidney.

To assess the contribution of the spleen to the induction of anti-*Candida* innate immunity after systemic *C. albicans* infection, we performed experiments in mice splenectomized 4 weeks before infection (Figure 7A). Interestingly, at 24 hr post-infection, a marked increase in serum and kidney GM-CSF levels, comparable to that observed in C57BL/6 mice (see Figure 3E), was detectable in sham-operated mice, but not in splenectomized mice (Figure 7B). Of note, low serum GM-CSF levels were detectable both in non-infected sham-operated mice and non-infected splenectomized mice, probably due to the surgical procedure. Accordingly, in *C. albicans*-infected splenectomized mice, the low iNOS mRNA expression detected in MACS-sorted CD45$^+$ kidney infiltrating leukocytes was paralleled by a defective induction above the basal values of non-infected mice, of the candidacidal potential of blood neutrophils (Figures 7C and 7D). As expected, the kidney fungal burden was significantly higher in splenectomized mice (Figure 7E), and consequently the survival of splenectomized mice was severely compromised (Figure 7F). These data demonstrate that the early innate immune response against *C. albicans* occurring in the spleen plays a crucial role in the induction of the immune mechanisms responsible to *Candida* clearance in the kidney, and thus in defense against systemic candidiasis. On the other hand, the fact that the reduction in GM-CSF production and neutrophil *Candida* killing ability, as well as the increase in kidney fungal load were similar when *Ccr2*$^{-/-}$ mice were compared to WT mice, and when splenectomized mice were compared to the sham-operated mice, supports that the main contribution of the spleen to innate immunity against systemic candidiasis during the first phases of infection, was to drive the activation and GM-CSF production by NK cells and subsequently to boost the candidacidal potential of neutrophils, through the production of IL-15 by spleen inflammatory Ly6C^{high} monocytes.

DISCUSSION

The cytokine IL-15 is known to be crucial for NK cell development (Di Santo, 2006), and for NK cell activation in defense against tumors and parasitic and microbial infections (Perera et al., 2012). Our studies have revealed a role for IL-15 as a critical mediator in defense against systemic candidiasis. We found that IL-15 is crucial for the activation and GM-CSF production by NK cells, which is required to boost the candidacidal potential of neutrophils and *Candida* clearance (Bär et al., 2014).

Analyses of the intracellular expression of the IL-15 trans-presenting receptor IL-15Rα, which reflect the production of IL-15 (Mortier et al., 2008), revealed that during *C. albicans* infection inflammatory Ly6C^{high} monocytes constituted the main IL-15-producing population, both in the spleen, an organ rapidly and transiently infected by *C. albicans*, and in the kidney, the main *Candida* target organ. Since at 24 hr post infection, the spleen harbored approximately 30-fold more IL-15Rα$^+$ Ly6C^{high} monocytes than the kidney, our findings suggest that spleen Ly6C^{high} monocytes are the major IL-15-producing cell population during *C. albicans* infection. We found that resident MØs and cDCs also contributed to IL-15 production after *C. albicans* infection, which is in line with previous studies showing that monocytes, MØs, and cDCs (Perera et al., 2012) produce IL-15 during viral and bacterial infections. Mice deficient for CCR2 displayed impaired recruitment of Ly6C^{high} inflammatory monocytes to the spleen and kidney. In these mice, blockade of IL-15 production, NK cell activation, GM-CSF production and neutrophil *Candida* killing ability can be reverted by the transfer of WT, but not of *Il15*$^{-/-}$ Ly6C^{high} monocytes. Moreover, in vitro production of GM-CSF by NK cells in response to *Candida* was dependent on IL-15 production by Ly6C^{high} monocytes. Taken together, these results demonstrate that the production of GM-CSF by activated NK cells that boost the *Candida* killing potential of neutrophils is largely dependent on the production of IL-15 by inflammatory Ly6C^{high} monocytes, therefore showing a pivotal function for Ly6C^{high} monocytes in the induction of innate defense mechanisms during systemic candidiasis. In this regard, our data concur with recent reports demonstrating that inflammatory monocytes play a critical role in the activation of effector cells that are in turn responsible for pathogen clearance.

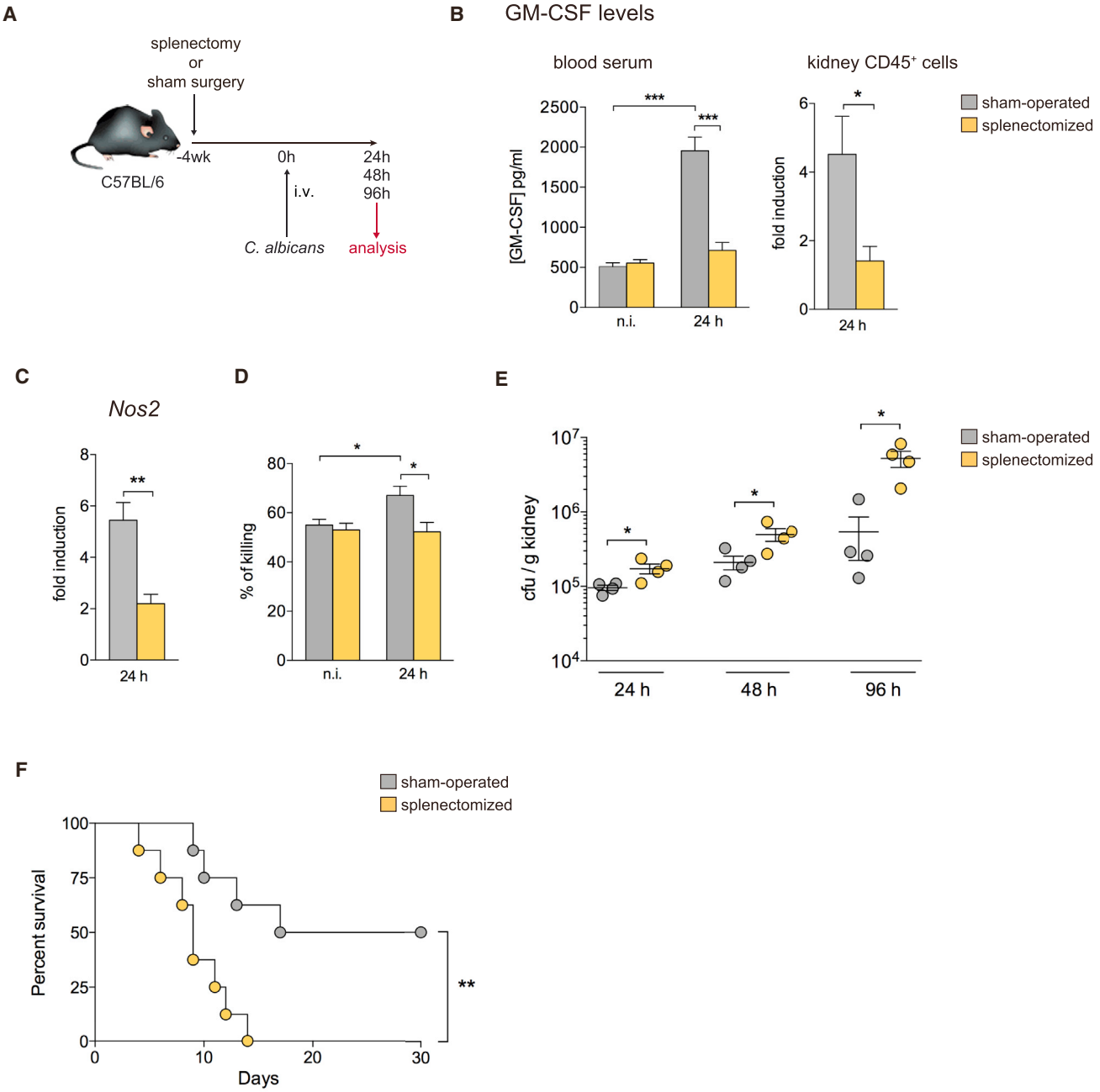

Figure 7. Contribution of the Spleen to the Induction of anti-*Candida* Innate Immunity during Systemic *C. albicans* Infection

(A) Protocol of splenectomy and *C. albicans* infection in C57BL/6 mice.

(B) GM-CSF analyzed by ELISA in blood serum, and by real-time PCR normalized to β-actin in MACS-sorted CD45$^+$ kidney infiltrating leukocytes, from sham-operated or splenectomized mice at the indicated times after *C. albicans* infection. Real-time PCR data are expressed as fold induction relative to non-infected mice.

(C) Expression of mRNA for iNOS by MACS-sorted CD45$^+$ kidney infiltrating leukocytes.

from sham-operated or splenectomized mice analyzed by real-time PCR, normalized to β-actin, at 24 hr after infection. Real-time PCR data are expressed as fold induction relative to non-infected mice.

(D) Candidacidal activity of blood neutrophils isolated from sham-operated or splenectomized mice at the indicated times after *C. albicans* infection.

(E) Kidney fungal burden of sham-operated or splenectomized mice at the indicated times after *C. albicans* infection.

(F) Survival of sham-operated or splenectomized mice after infection. Data are presented as a Kaplan-Maier plot with a log rank test used to compare susceptibility between the two groups. n = 8. Data are expressed as mean ± SEM of four mice per condition. *p < 0.05; **p < 0.01; ***p < 0.001; unpaired t test. Similar results were obtained in three independent experiments. i.v. intravenous; n.i., non-infected.

Production of IL-18 and IL-15 by Ly6C^{high} inflammatory monocytes is crucial for the activation of CD8^{+} T cells and NK cells during *Listeria* infection (Soudja et al., 2012), and *Klebsiella* clearance requires TNFα production by Ly6C^{high} inflammatory monocytes, which in turn drives IL-17A production by innate lymphoid cells (Xiong et al., 2016).

However, the relevance of IL-15 production by inflammatory Ly6C^{high} monocytes for NK cell activation during systemic candidiasis had not been explored before, and few studies have addressed the mechanism of NK activation after *C. albicans* infection. IL-15 was reported to increase the in vitro microbicidal potential of human neutrophils (Musso et al., 1998) and monocytes (Vázquez et al., 1998) in response to *C. albicans*. Regarding NK cell activation, IL-23 was proposed to participate in NK activation during *C. albicans* infection (Whitney et al., 2014) although whether this cytokine controls the activation of NK cells in the spleen was not addressed in this report.

In line with published data demonstrating that IL-15 synthesis after in vitro TLR engagement (Lucas et al., 2007) or in vivo viral infection (Colpitts et al., 2012) is dependent on IFNAR signaling, our data revealed that the production of IL-15 in response to *C. albicans* infection was suppressed in *Ifnar1*$^{-/-}$ mice, and thus that type I IFN production was required for the production of IL-15 during systemic candidiasis. Our group has previously shown that dectin/Syk/IRF5-dependent type I IFN production is crucial for defense against *C. albicans* infection (del Fresno et al., 2013). The IFNAR dependency for IL-15 production in response to *C. albicans* further supports the relevance of type I IFN production during fungal infections. Our results can also provide a potential explanation for the detrimental effect of type I IFN during *C. albicans* infection reported by the group of Kuchler and colleagues (Majer et al., 2012), since excessive type I IFN-dependent IL-15 production might trigger an exacerbated activation of the NK cell-neutrophil axis, which could ultimately lead to neutrophil-mediated inflammatory pathology and reduced host survival.

In mice, systemic candidiasis caused by intravenous *Candida* infection leads to the dissemination of the fungus to a number of organs including the spleen, liver and brain, which harbor low fungal loads and are as a result only transiently infected (Lionakis et al., 2011). The kidney is the main *Candida* target organ, and can harbor large fungal loads paralleled by hypha formation, which can lead ultimately lead to fatal renal failure (Netea et al., 2015). Based on the pathogenesis of invasive candidiasis, research efforts have focused on exploring the induction of anti-*Candida* immunological defense mechanisms in the kidney. However, at steady state the kidney immune system is limited mainly to a population of resident MØs and a low number of monocytes, DCs, and lymphocytes (Kurts et al., 2013); the kidney is not well prepared to mount an effective immune response during infectious processes. Our findings provide evidence supporting a pivotal collaborative function for the spleen in the establishment of anti-*Candida* immunity, wherein the spleen provides crucial help in order to achieve an effective immune response in the kidney during *C. albicans* infection. The efficient innate immune system of the spleen ensures the rapid clearance of *Candida* during the first hours after infection, enabling a robust spleen Ly6C^{high} monocyte-driven IL-15 production that leads to the activation of large numbers of splenic NK cells and to the production of large amounts of GM-CSF, which are in turn required to boost the neutrophil *Candida* killing capacity in the kidney.

In conclusion, the present study provides strong evidence that type-I IFN dependent-IL-15 production plays a decisive function during invasive candidiasis by driving spleen NK cell activation and GM-CSF production that enables kidney neutrophils to control fungal growth. Our data therefore reinforce previous studies on the relevance of type-I IFN in antifungal immunity (McNab et al., 2015), and on the key role fulfilled by NK cells in defense against systemic candidiasis (Bär et al., 2014). However further research should be conducted to explore additional functions of type-I IFN in candidiasis, and to define the immune cell types responsible for its production after systemic *C. albicans* infection. Importantly, the evidence presented here on the pivotal role played by IL-15 in defense against *C. albicans* could set the basis for the design of potent IL-15-based immunotherapeutic strategies against fungal infections. In this regard, the development of new antifungal immunotherapies is urgently needed due to the emergence of multidrug-resistant *Candida* species, such as *Candida auris*, causing serious invasive infections (McCarthy and Walsh, 2017), and to the relative low efficiency of antifungal chemotherapy in patients receiving immunosuppressive treatments (Kullberg and Arendrup, 2015).

STAR★METHODS

Detailed methods are provided in the online version of this paper and include the following:

- KEY RESOURCES TABLE
- CONTACT FOR REAGENTS AND RESOURCE SHARING
- EXPERIMENTAL MODEL
  - Mice
- METHOD DETAILS
  - Mouse model of systemic candidiasis
  - Fungal Burden Determination
  - Kidney and Spleen Cell Suspensions
  - Isolation of Cell Populations
  - Flow Cytometry
  - Neutrophil Killing Assays
  - RNA Extraction and Real-Time PCR
  - Analysis of Cytokine Production
  - Histology
  - Monocyte-NK Cell Cocultures
  - In Vivo Treatment with IL-15
  - In Vivo Treatment with anti-IL-15Rα/IL-15 Antibody
  - Monocyte Transfer Experiments
  - Splenectomy
  - Culture and Stimulation of BMDCs
- QUANTIFICATION AND STATISTICAL ANALYSIS

SUPPLEMENTAL INFORMATION

Supplemental Information includes seven figures and one table and can be found with this article online at http://dx.doi.org/10.1016/j.immuni.2017.05.009.

AUTHOR CONTRIBUTIONS

C.A. designed the research, analyzed the data and wrote the manuscript. J.D.-A. designed the research, analyzed the data, and prepared the manuscript. J.D.-A.,

L.F.-L., M.M.E. and L.G. performed the experiments. M.L.-B. contributed to experimental design and data analysis.

ACKNOWLEDGMENTS

We thank C. Gil for *C. albicans* SC5314 strain and experimental advice. F. Tacke for *Ccr2*$^{-/-}$ mice, J. di Santo for *Il15*$^{-/-}$ mice, U. Kalinke for *Ifnar1*$^{-/-}$ mice, G. Brown for *Clec7a*$^{-/-}$ bone marrow, I. Udalova for *Irf5*$^{-/-}$ bone marrow and S. Colpitts, C. del Fresno, S. Leibundgut-Landmann, A. Marçais, L. Puddington, D. Sancho, and T. Walzer for scientific advice. J.D.-A. received a La Caixa Foundation PhD fellowship. This work was supported by the Spanish Ministerio de Economía y Competitividad (Grants SAF 2012-35670 and SAF2015-69905) to C.A.

Received: December 13, 2016
Revised: March 16, 2017
Accepted: April 19, 2017
Published: June 20, 2017

REFERENCES

Bär, E., Whitney, P.G., Moor, K., Reis e Sousa, C., and LeibundGut-Landmann, S. (2014). IL-17 regulates systemic fungal immunity by controlling the functional competence of NK cells. Immunity *40*, 117–127.

Colpitts, S.L., Stoklasek, T.A., Plumlee, C.R., Obar, J.J., Guo, C., and Lefrançois, L. (2012). Cutting edge: the role of IFN-α receptor and MyD88 signaling in induction of IL-15 expression in vivo. J. Immunol. *188*, 2483–2487.

del Fresno, C., Soulat, D., Roth, S., Blazek, K., Udalova, I., Sancho, D., Ruland, J., and Ardavín, C. (2013). Interferon-β Production via Dectin-1-Syk-IRF5 Signaling in Dendritic Cells is Crucial for Immunity to C. albicans. Immunity 38, no. 6 (2013): 1176-1186. Immunity *38*, 1176–1186.

Di Santo, J.P. (2006). Natural killer cell developmental pathways: a question of balance. Annu. Rev. Immunol. *24*, 257–286.

Ebihara, T., Azuma, M., Oshiumi, H., Kasamatsu, J., Iwabuchi, K., Matsumoto, K., Saito, H., Taniguchi, T., Matsumoto, M., Seya, T., et al. (2010). Identification of a polyI:C-inducible membrane protein that participates in dendritic cell-mediated natural killer cell activation. J. Exp. Med. *207*, 2675–2687.

Engel, D.R., Maurer, J., Tittel, A.P., Weisheit, C., Cavlar, T., Schumak, B., Limmer, A., van Rooijen, N., Trautwein, C., Tacke, F., et al. (2008). CCR2 mediates homeostatic and inflammatory release of Gr1(high) monocytes from the bone marrow, but is dispensable for bladder infiltration in bacterial urinary tract infection. J. Immunol. *181*, 5579–5586.

Frenz, T., Waibler, Z., Hofmann, J., Hamdorf, M., Lantermann, M., Reizis, B., Tovey, M.G., Aichele, P., Sutter, G., and Kalinke, U. (2010). Concomitant type I IFN receptor-triggering of T cells and of DC is required to promote maximal modified vaccinia virus Ankara-induced T-cell expansion. Eur. J. Immunol. *40*, 2769–2777.

Hernández-Santos, N., and Gaffen, S.L. (2012). Th17 cells in immunity to Candida albicans. Cell Host Microbe *11*, 425–435.

Horowitz, A., Stegmann, K.A., and Riley, E.M. (2012). Activation of natural killer cells during microbial infections. Front. Immunol. *2*, 88.

Iliev, I.D., Funari, V.A., Taylor, K.D., Nguyen, Q., Reyes, C.N., Strom, S.P., Brown, J., Becker, C.A., Fleshner, P.R., Dubinsky, M., et al. (2012). Interactions between commensal fungi and the C-type lectin receptor Dectin-1 influence colitis. Science *336*, 1314–1317.

Kanafani, Z.A., and Perfect, J.R. (2008). Antimicrobial resistance: resistance to antifungal agents: mechanisms and clinical impact. Clin. Infect. Dis. *46*, 120–128.

Krausgruber, T., Blazek, K., Smallie, T., Alzabin, S., Lockstone, H., Sahgal, N., Hussell, T., Feldmann, M., and Udalova, I.A. (2011). IRF5 promotes inflammatory macrophage polarization and TH1-TH17 responses. Nat. Immunol. *12*, 231–238.

Kullberg, B.J., and Arendrup, M.C. (2015). Invasive Candidiasis. N. Engl. J. Med. *373*, 1445–1456.

Kurts, C., Panzer, U., Anders, H.-J., and Rees, A.J. (2013). The immune system and kidney disease: basic concepts and clinical implications. Nat. Rev. Immunol. *13*, 738–753.

Lionakis, M.S., Lim, J.K., Lee, C.-C.R., and Murphy, P.M. (2011). Organ-specific innate immune responses in a mouse model of invasive candidiasis. J. Innate Immun. *3*, 180–199.

Lucas, M., Schachterle, W., Oberle, K., Aichele, P., and Diefenbach, A. (2007). Dendritic cells prime natural killer cells by trans-presenting interleukin 15. Immunity *26*, 503–517.

Majer, O., Bourgeois, C., Zwolanek, F., Lassnig, C., Kerjaschki, D., Mack, M., Müller, M., Kuchler, K., Wisplinghoff, H., Seifert, H., et al. (2012). Type I interferons promote fatal immunopathology by regulating inflammatory monocytes and neutrophils during Candida infections. PLoS Pathog. *8*, e1002811.

Marçais, A., Viel, S., Grau, M., Henry, T., Marvel, J., and Walzer, T. (2013). Regulation of mouse NK cell development and function by cytokines. Front. Immunol. *4*, 450.

McCarthy, M.W., and Walsh, T.J. (2017). Drug development challenges and strategies to address emerging and resistant fungal pathogens. Expert Rev. Anti Infect. Ther. *15*, 577–584.

McNab, F., Mayer-Barber, K., Sher, A., Wack, A., and O'Garra, A. (2015). Type I interferons in infectious disease. Nat. Rev. Immunol. *15*, 87–103.

Mortier, E., Woo, T., Advincula, R., Gozalo, S., and Ma, A. (2008). IL-15Ralpha chaperones IL-15 to stable dendritic cell membrane complexes that activate NK cells via trans presentation. J. Exp. Med. *205*, 1213–1225.

Musso, T., Calosso, L., Zucca, M., Millesimo, M., Puliti, M., Bulfone-Paus, S., Merlino, C., Savoia, D., Cavallo, R., Ponzi, A.N., and Badolato, R. (1998). Interleukin-15 activates proinflammatory and antimicrobial functions in polymorphonuclear cells. Infect. Immun. *66*, 2640–2647.

Naglik, J.R. (2014). Candida Immunity. New J. Sci. *2014*, 1–27.

Netea, M.G., Brown, G.D., Kullberg, B.J., and Gow, N.A.R. (2008). An integrated model of the recognition of Candida albicans by the innate immune system. Nat. Rev. Microbiol. *6*, 67–78.

Netea, M.G., Joosten, L.A.B., van der Meer, J.W.M., Kullberg, B.-J., and van de Veerdonk, F.L. (2015). Immune defence against Candida fungal infections. Nat. Rev. Immunol. *15*, 630–642.

Ngo, L.Y., Kasahara, S., Kumasaka, D.K., Knoblaugh, S.E., Jhingran, A., and Hohl, T.M. (2014). Inflammatory monocytes mediate early and organ-specific innate defense during systemic candidiasis. J. Infect. Dis. *209*, 109–119.

Perera, P.-Y., Lichy, J.H., Waldmann, T.A., and Perera, L.P. (2012). The role of interleukin-15 in inflammation and immune responses to infection: implications for its therapeutic use. Microbes Infect. *14*, 247–261.

Reales-Calderón, J.A., Martínez-Solano, L., Martínez-Gomariz, M., Nombela, C., Molero, G., and Gil, C. (2012). Sub-proteomic study on macrophage response to Candida albicans unravels new proteins involved in the host defense against the fungus. J. Proteomics *75*, 4734–4746.

Shi, C., and Pamer, E.G. (2011). Monocyte recruitment during infection and inflammation. Nat. Rev. Immunol. *11*, 762–774.

Soudja, S.M., Ruiz, A.L., Marie, J.C., and Lauvau, G. (2012). Inflammatory monocytes activate memory CD8(+) T and innate NK lymphocytes independent of cognate antigen during microbial pathogen invasion. Immunity *37*, 549–562.

Vázquez, N., Walsh, T.J., Friedman, D., Chanock, S.J., and Lyman, C.A. (1998). Interleukin-15 augments superoxide production and microbicidal activity of human monocytes against Candida albicans. Infect. Immun. *66*, 145–150.

Whitney, P.G., Bär, E., Osorio, F., Rogers, N.C., Schraml, B.U., Deddouche, S., LeibundGut-Landmann, S., and Reis e Sousa, C. (2014). Syk signaling in dendritic cells orchestrates innate resistance to systemic fungal infection. PLoS Pathog. *10*, e1004276.

Xiong, H., Keith, J.W., Samilo, D.W., Carter, R.A., Leiner, I.M., Pamer, E.G., Abt, M.C., Lewis, B.B., Caballero, S., Xiong, H., et al. (2016). Innate Lymphocyte/Ly6C(hi) Monocyte Crosstalk Promotes Klebsiella Pneumoniae Clearance. Cell *165*, 679–689.

STAR★METHODS

KEY RESOURCES TABLE

REAGENT or RESOURCE	SOURCE	IDENTIFIER
Antibodies		
Biotin-conjugated anti-CD45	CIEMAT	N/A
Biotin-conjugated anti-CD11b	Ludwig Institute for Cancer Research	N/A
Biotin-conjugated anti-Ly6G	BioLegend	Cat#127603; RRID: AB_1186105
Anti-CD49b (DX5)-microbeads	Miltenyi Biotec	Cat#130-052-501
Anti-rat immunoglobulin-coated magnetic beads	ThermoFischer	Cat#11035
Anti-mouse immunoglobulin-coated magnetic beads	ThermoFischer	Cat#11031
Anti-Thy 1.2	Ludwig Institute for Cancer Research	N/A
Anti-B220	Ludwig Institute for Cancer Research	N/A
Anti-MHC-II	Ludwig Institute for Cancer Research	N/A
Anti-CD43	CBMSO	N/A
Anti-CD24	Ludwig Institute for Cancer Research	N/A
Anti-Ly6G	BioXCell	Cat#BE0075-1; RRID: AB_1107721
FITC-conjugated anti-MHCII	BD PharMingen	Cat#553623; RRID: AB_394958
PECy7-conjugated anti-CD11b	BD PharMingen	Cat#552850; RRID: AB_394491
APC-conjugated anti-CD64	Biolegend	Cat#139305; RRID: AB_11219205
APC-Cy7-conjugated anti-CD11c	BD PharMingen	Cat#561241; RRID: AB_10611727
PE-conjugated anti-CD49b	Biolegend	Cat#103506; RRID: AB_313029
PE-conjugated anti-CD90	BD PharMingen	Cat#553005; RRID: AB_394544
PE-conjugated anti-CD19	BD PharMingen	Cat#555413; RRID: AB_395813
Pacific Blue-conjugated anti-CD45	Biolegend	Cat#103125; RRID: AB_493536
Biotin-conjugated anti-Ly6C	BioXCell	Cat# BE0203
Streptavidin-PerCP	BD PharMingen	Cat#554064; RRID: AB_2336918
APC-eFluor780-conjugated anti-CD3	eBioscience	Cat#47-0038-41; RRID: AB_1272112
APC-conjugated anti-IFN-γ	BD PharMingen	Cat#554413; RRID: AB_398551
PECy7 conjugated anti-GrB	eBioscience	Cat#25-8898;RRID: AB_10853338
FITC-conjugated anti-CD122 (eBioscience)	eBioscience	Cat#123207; RRID: AB_940611
Biotin-conjugated anti-CD49b	eBioscience	Cat#108903; RRID: AB_313410
Anti-FcγRII/III	Ludwig Institute for Cancer Research	N/A
Biotin-conjugated anti-CD11c	Ludwig Institute for Cancer Research	N/A
Anti-IL-15R/IL-15 blocking antibody	eBioscience	Cat#16-8156-82
Fungal Strains		
C. albicans SC5314 strain	Dr. Concha Gil (Reales-Calderón et al., 2012)	ATCC MYA-2876
Chemicals, Peptides, and Recombinant Proteins		
Liberase TM Research grade	Roche	Cat#05401119001
DNase I	Roche	Cat#04716728001
Ficoll-Paque Plus	GE Healthcare	● Cat#17-1440-02
Collagenase A	Roche	Cat#010103578001
Streptavidin Microbeads	Miltenyi Biotech	Cat#130-048-102
Histopaque 1077	Sigma	Cat#10771
Histopaque 1119	Sigma	Cat#11191
LPS from *Escherichia coli*	Sigma	Cat#L2630
Fibronectin	Sigma	Cat#F1141
Recombinant mouse IL-15	Peprotech	Cat#210-15

(*Continued on next page*)

Continued		
REAGENT or RESOURCE	SOURCE	IDENTIFIER
Recombinant GM-CSF	Peprotech	Cat#315-03
Curdlan	Wako	Cat#034-09901
Critical Commercial Assays		
Murine GM-CSF Standard ABTS ELISA Development Kit	Peprotech	Cat#900-K55
BD OptEIA Mouse IFNγ ELISA Set	BD Biosciences	Cat#555138
RNAqueous-Micro kit	Ambion	Cat#AM1931
High Pure RNA Isolation kit	Roche	Cat#11828665001
High Capacity cDNA Reverse Transcription kit	Applied	Cat#4368814
5x HOT FIREPol EvaGreen qPCR Mix Plus	Solis	Cat#08-24-00001
Experimental Models: Organisms/Strains		
C57BL/6 mice	Charles River	JAX000664
Ccr2$^{-/-}$ mice	Dr. Frank Tacke Engel et al. (2008)	N/A
Il15$^{-/-}$ mice	Dr. James di Santo (Ebihara et al., 2010)	N/A
Ifnar1$^{-/-}$ mice	Dr. Ulrich Kalinke (Frenz et al., 2010)	N/A
Clec7a$^{-/-}$ mice, bone marrow	Dr. Gordon Brown (Iliev et al., 2012)	N/A
Irf5$^{-/-}$ mice, bone marrow	Dr. Irina Udalova (Krausgruber et al., 2011).	N/A
Software and Algorithms		
GraphPad Prism 6	GraphPad Software Inc	http://www.graphpad.com/scientific-software/prism/
FlowJo X	FlowJo	https://www.flowjo.com/solutions/flowjo
Other		
BD LSR II Flow Cytometer	BD Biosciences	N/A
Oligonucleotides		
See Table S1 for Real-Time PCR primer sequences		

CONTACT FOR REAGENTS AND RESOURCE SHARING

Further information and requests for reagents may be directed to the Lead contact Carlos Ardavín (ardavin@cnb.csic.es).

EXPERIMENTAL MODEL

Mice

C57BL/6 mice were purchased from Charles River (L'Arbresle, France). *Ccr2*$^{-/-}$ mice were kindly supplied by Dr. F. Tacke (RWTH-University Hospital Aachen, Aachen, Germany). *Ifnar1*$^{-/-}$ mice were kindly provided by Dr. U. Kalinke (Center for Experimental and Clinical Infection Research, Hannover, Germany). *Il15*$^{-/-}$ mice were kindly supplied by Dr. J. di Santo (Institut Pasteur, Paris, France). 8 to 12-week old C57BL/6, *Ccr2*$^{-/-}$, *Ifnar1*$^{-/-}$ and *Il15*$^{-/-}$ mice were housed at the Animal Facility of the Centro Nacional de Biotecnología/CSIC, Madrid, Spain, on a 12 hr/12 hr light/dark cycle, with free access to food and water. Littermates of the same sex were randomly assigned to experimental groups. Bone marrow from *Clec7a*$^{-/-}$ mice was kindly provided by Dr. G. Brown (University of Aberdeen, Aberdeen, UK). Bone marrow from *Irf5*$^{-/-}$ mice was kindly provided by Dr. I. Udalova (Kennedy Institute of Rheumatology, University of Oxford, Oxford, UK). All the experiments were approved by the Animal Care and Use Committee of the Centro Nacional de Biotecnología-CSIC, Madrid, under the protocol number 312.14

METHOD DETAILS

Mouse model of systemic candidiasis

C. albicans (strain SC5314; kindly provided by Dr. C. Gil, Complutense University, Madrid) was grown on YPD plates (Sigma-Aldrich, St Louis, MO) at 30°C. *C. albicans* cells were centrifuged, washed in PBS and counted using a hematocytometer. Mice were infected by intravenous injection of 1 x 10^5 *C. albicans* via the lateral tail vein and monitored daily for health and survival following the institutional guidance. HKC were obtained by incubation of *C. albicans,* strain SC5314, for 30 min at 100°C.

Fungal Burden Determination

Organs were aseptically removed, weighed and homogenized in PBS using a T10 basic Ultra-Turrax homogenizer (Ika, Staufen, Germany). Fungal burden was determined by plating organ homogenates in serial dilutions on YPD plates. Colony forming units (CFUs) were counted after growth for 48 hr at 30°C.

Kidney and Spleen Cell Suspensions

Analysis of renal leukocyte infiltrates was performed on cell suspensions obtained from organ homogenates that were digested with 0.2 mg/ml of Liberase TM (Roche, Mannheim, Germany) and 40 mg/ml of DNase I (Roche) for 20 min at 37°C, filtered through 40-μm cell strainers (BD PharMingen, San Diego, CA) and washed twice in EDTA-containing PBS, after erythrocyte lysis by osmotic shock. Then cells were centrifuged on a Ficoll-Paque Plus gradient (GE Healthcare, Uppsala, Sweden) for 20 min at 700 g. Analysis of splenic leukocytic infiltrates was performed on cell suspensions obtained from organ homogenates that were digested with 0.5 mg/ml of Collagenase I (Roche) and 40 mg/ml of DNase I for 10 min at 37°C, filtered through 40-μm cell strainers and washed twice in EDTA-containing PBS after erythrocyte lysis by osmotic shock.

Isolation of Cell Populations

Kidney infiltrating leukocytes were purified by immunomagnetic positive selection after incubation with biotin-conjugated anti-CD45, followed by streptavidin-conjugated microbeads (Miltenyi Biotech). Spleen CD11b$^+$ NK and myeloid cells were purified by immunomagnetic positive selection after incubation with biotin-conjugated anti-CD11b followed by streptavidin-conjugated microbeads. Kidney neutrophils were purified by immunomagnetic positive selection after incubation with biotin-conjugated anti-Ly6G, followed by streptavidin-conjugated microbeads. Circulating neutrophils were isolated from blood drawn by cardiac puncture, diluted in PBS containing 5 mM EDTA and 3% FCS, overlaid over a density gradient of Histopaque 1119 and Histopaque 1077 (Sigma) and centrifuged for 30 min at 400 g. Neutrophil preparations had a purity > 80%. Spleen NK cells were purified after incubation with anti-CD49b (DX5)-conjugated microbeads (Miltenyi Biotech). NK cell preparations had a purity > 95%. Monocytes were isolated from lysis buffer–treated bone marrow cell suspensions by using immunomagnetic depletion of T cells, B cells, DCs, granulocytes and natural killer cells with anti-rat immunoglobulin-coated magnetic beads (Invitrogen, Karlsruhe, Germany) at a 7:1 bead-to-cell ratio after incubation with the mAbs anti–Thy-1.2, B220, MHC-II, CD43, CD24 and Ly6G. After immunomagnetic depletion, monocyte preparations had a purity > 90%.

Flow Cytometry

Analysis of kidney and spleen cell suspensions was performed after seven-color staining using FITC-conjugated anti-MHCII (BD PharMingen), PECy7-conjugated anti-CD11b (BD PharMingen), APC-conjugated anti-CD64 (Biolegend, San Diego, CA), APC-Cy7-conjugated anti-CD11c (BD PharMingen), PE-conjugated anti-Ly6G (BD PharMingen), PE-conjugated anti-Siglec-F (BD PharMingen), PE-conjugated anti-CD49b (Biolegend), PE-conjugated anti-CD90 (BD PharMingen) and PE-conjugated anti-CD19 (BD PharMingen), Pacific Blue-conjugated anti-CD45 (Biolegend) and biotin-conjugated anti-Ly6C, followed by streptavidin-PerCP (BD PharMingen). Antibodies anti-Ly6G, Siglec-F, CD49b, CD90 and CD19 were used together as PE-conjugates with the purpose of gating out neutrophils, eosinophils, NK cells, T cells and B cells, respectively. For the detection of IFN-γ and Granzyme B (GrB) production by NK cells in spleen and kidney cell suspensions, cells were first stained with PE-conjugated anti-CD49b (Biolegend), APC-eFluor780-conjugated anti-CD3 (eBioscience) and Pacific Blue-conjugated anti-CD45, and subsequently stained with APC-conjugated anti-IFN-γ (BD PharMingen) and PECy7-conjugated anti-GrB (eBioscience) after 4% paraformaldehyde fixation and permeabilization with 0.3% saponin and 0.5% bovin serum albumin BSA (Sigma). For the detection of CD122 expression by NK cells and neutrophils in spleen and kidney cell suspensions, cells were stained with FITC-conjugated anti-CD122 (eBioscience), PE-conjugated anti-Ly6G, APC-eFluor780-conjugated anti-CD3, Pacific Blue-conjugated anti-CD45 and biotin-conjugated anti-CD49b, followed by streptavidin-PerCP. Fc receptors were blocked with anti-FcγRII/III mAbs (clone 2.4G2). Data were acquired on a LSRII cytometer (BD Biosciences, San José, CA) and analyzed using FlowJo X software (Tree Star, Ashland, OR).

Neutrophil Killing Assays

To test neutrophil killing activity, 10^4 *C. albicans* cells were exposed to 5×10^4 neutrophils for 2 hr; neutrophils were then lysed with water and the number of surviving yeast cells was assessed on YPD agar. Killing activity was expressed as percentage of *C. albicans* cells surviving in the presence of neutrophils compared to *C. albicans* cells surviving in the absence of neutrophils.

RNA Extraction and Real-Time PCR

For real-time PCR analyses, RNA from kidney inflitrating leukocytes, spleen CD11b$^+$ NK and myeloid cells, purified kidney neutrophils or purified spleen NK cells was extracted using the RNAqueous-Micro kit (Ambion, Austin, TX). RNA from BMDCs was extracted using the High Pure RNA Isolation kit (Roche). RNA was retro-transcribed using the High Capacity cDNA Reverse Transcription kit (Applied Biosystems, Carlsbad, CA). Real-time PCR was performed using 5x HOT FIREPol EvaGreen qPCR Mix Plus (Solis BioDyne, Tartu, Estonia) on an ABI PRISM 7900 Sequence Detection System (Applied Biosystems). Primer sequences are listed in Table S1.

Analysis of Cytokine Production

Production of GM-CSF in serum and cell culture supernatants was measured using murine GM-CSF Standard ABTS ELISA Development Kit (Peprotech). IFNγ production in culture supernatants was measured using BD OptEIA Mouse IFNγ ELISA Set (BD Biosciences).

Histology

Kidneys were fixed with 4% paraformaldehyde and embedded in paraffin. 5 μm-sections were stained with periodic-acid Schiff (PAS) and counterstained with hematoxylin. Images were acquired with a Leica FDM2500 microscope (Leica, Wetzlar, Germany).

Monocyte-NK Cell Cocultures

1 x 10^5 purified bone marrow monocytes, stimulated with 100 ng/ml LPS from *Escherichia coli* (Sigma) or 5 x 10^5/ml HKC, for 6 hours, were cultured with 1 x 10^5 purified spleen NK cells, in fibronectin-coated, tissue culture-treated, flat-bottom 96 well plates (Corning, Durham, NC), in complete RPMI 1640 medium supplemented with 10% FCS, 2 mM L-glutamine, 100 U/ml penicillin, 100 μg/ml streptomycin and 50 μM 2-mercaptoethanol, for 18 hours at 37°C. GM-CSF and IFNγ production was measured in culture supernatants by ELISA as described above.

In Vivo Treatment with IL-15

Mice were injected intraperitoneally for two consecutive days with 0.5 μg recombinant mouse IL-15 (Peprotech), or PBS, prior to an intravenous injection with 1 × 10^5 *C. albicans* cells.

In Vivo Treatment with anti-IL-15Rα/IL-15 Antibody

Mice were injected intraperitoneally with 15 μg of an anti-IL-15Rα/IL-15 blocking antibody (eBioscience, San Diego, CA), or an isotype control antibody, concomitantly with an intravenous injection of 1 × 10^5 *C. albicans* cells.

Monocyte Transfer Experiments

4 x 10^6 bone marrow monocytes isolated from *Il15*$^{-/-}$, *Ifnar1*$^{-/-}$, or WT CD45.1$^+$ C57BL/6 mice (purchased from Jackson, Maine, USA) were transferred intravenously into CD45.2$^+$ *Ccr2*$^{-/-}$ mice that received concomitantly an intravenous injection with 1 x 10^5 *C. albicans* cells.

Splenectomy

Mice were anesthetized with an intraperitoenal injection of ketamine (100 mg/kg) and xylazine (10 mg/kg). For splenectomy, the skin above the spleen was prepared for surgery by depilation and contact sterilization, the abdominal wall was opened through a subcostal abdominal incision, the splenic hilar vessels were ligated with 4–0 silk, the spleen was removed, and the abdominal incision was closed. In sham-operated mice, the same procedure was employed to open the abdominal wall that was closed immediately after identifying the spleen.

Culture and Stimulation of BMDCs

BMDCs were obtained from bone marrow cell suspensions after culture on non-treated culture 150-mm Petri dishes in complete RPMI 1640 medium supplemented with 10% FCS, 2 mM L-glutamine, 100 U/ml penicillin, 100 μg/ml streptomycin, 50 μM 2-mercaptoethanol and 20 ng/ml recombinant GM-CSF (Peprotech). Cells were collected at day 8, and BMDCs were purified by immunomagnetic positive selection after incubation with biotin-conjugated anti-CD11c and streptavidin-conjugated microbeads. Preparations of BMDCs, characterized as CD11c$^+$ MHCII$^+$ cells, had a purity > 95%. BMDCs were rested for 6 hr in complete cell culture medium and subsequently stimulated at the indicated times with 100 ng/ml LPS from *Escherichia coli*, 10 μg/ml Curdlan (Wako chemicals, Neuss, Germany), or 5 × 10^5/ml HKC.

QUANTIFICATION AND STATISTICAL ANALYSIS

Data are presented as mean ± SEM, as indicated in the legend of each figure. The significance of the differences between groups was evaluated using unpaired t test, p value < 0.05 was considered significant. Survival curve data are presented as a Kaplan-Maier plot with a log rank test used to compare susceptibility between the two groups, p value < 0.05 was considered significant. Statistical parameters including the exact value of n, precision measures (mean ± SEM) and statistical significance are reported in the Figures and the Figure Legends when necessary. Data are judged to be statistically significant when p < 0.05 by two-tailed Student's t test. In figures, asterisks denote statistical significance (*, p < 0.05; **, p < 0.01; ***, p < 0.001). Statistical analysis was performed in GraphPad PRISM 6.